



OPEN ACCESS

EDITED BY

Christopher Edward Cornwall,
Victoria University of Wellington,
New Zealand

REVIEWED BY

Wei Liu,
Shanghai University, China
Kristian Spilling,
Finnish Environment Institute (SYKE), Finland

*CORRESPONDENCE

Marianne Camoying
✉ marianne.camoying@awi.de

RECEIVED 30 May 2024

ACCEPTED 09 October 2024

PUBLISHED 04 November 2024

CITATION

Camoying M, Koch F, Stimpfle J, Pausch F,
Hassler C and Trimbom S (2024) Distinct
responses of diatom- and flagellate-
dominated Antarctic phytoplankton
communities to altered iron and light supply.
Front. Mar. Sci. 11:1441087.
doi: 10.3389/fmars.2024.1441087

COPYRIGHT

© 2024 Camoying, Koch, Stimpfle, Pausch,
Hassler and Trimbom. This is an open-access
article distributed under the terms of the
[Creative Commons Attribution License \(CC BY\)](https://creativecommons.org/licenses/by/4.0/).
The use, distribution or reproduction in other
forums is permitted, provided the original
author(s) and the copyright owner(s) are
credited and that the original publication in
this journal is cited, in accordance with
accepted academic practice. No use,
distribution or reproduction is permitted
which does not comply with these terms.

Distinct responses of diatom- and flagellate-dominated Antarctic phytoplankton communities to altered iron and light supply

Marianne Camoying^{1*}, Florian Koch¹, Jasmin Stimpfle¹,
Franziska Pausch¹, Christel Hassler^{2,3} and Scarlett Trimbom¹

¹EcoTrace, Alfred Wegener Institute, Helmholtz Centre for Polar and Marine Research, Bremerhaven, Germany, ²Department F.-A. Forel for Environmental and Aquatic Science, University of Geneva, Geneva, Switzerland, ³Ecole Polytechnique Fédérale de Lausanne, Sion, Switzerland

Primary production in the Southern Ocean is strongly influenced by the availability of light and iron (Fe). To examine the response of two distinct natural Antarctic phytoplankton communities (diatom vs. flagellates) to increasing light and Fe availability, we conducted two shipboard incubation experiments during late summer and exposed each community to increasing light intensities (30, 80, and 150 $\mu\text{mol photons m}^{-2} \text{s}^{-1}$) with or without Fe amendment. Our results show clearly that both communities were Fe-limited since Fe addition resulted in higher particulate organic carbon (POC) production rates. The magnitude of the Fe-dependent increase in POC production, however, varied between the two stations being higher in the diatom-dominated community relative to the flagellate-dominated community. This differential response to increasing Fe supply could be attributed to the higher Fe requirement of the flagellate-dominated assemblage relative to the diatom-dominated assemblage. Irrespective of Fe availability, light also strongly stimulated the POC production of both communities between low and medium light supply (30 versus 80 $\mu\text{mol photons m}^{-2} \text{s}^{-1}$), indicating that both assemblages were light-limited *in situ*. However, since POC production of both communities did not increase further at the highest light intensity (150 $\mu\text{mol photons m}^{-2} \text{s}^{-1}$) even under high Fe supply, this suggests that light supply was saturated or that other conditions must be fulfilled (e.g., availability of trace metals other than Fe) in order for the communities to benefit from the higher light and Fe conditions.

KEYWORDS

Southern Ocean, diatoms, flagellates, light, iron, photoacclimation, ecophysiology, Fe demand

Introduction

Primary production in the Southern Ocean (SO) is mainly constrained by the availability of light and the trace metal iron (Fe; Martin et al., 1990; Mitchell et al., 1991; Strzpek et al., 2019). As Fe plays an important role in the cellular process of photosynthesis (Behrenfeld and Milligan, 2013), several studies have already established the positive effects of Fe addition on the growth and carbon production of SO phytoplankton (Boyd et al., 2000; Blain et al., 2007; Moore et al., 2007). The effect of Fe on SO phytoplankton is, however, influenced by light availability. An antagonistic relationship between Fe and light has been observed in temperate phytoplankton (Sunda and Huntsman, 1997; Maldonado et al., 1999) wherein the Fe demand is said to increase under low light conditions, amplifying thereby Fe limitation. In particular, at low irradiance, phytoplankton cells would require more Fe for the synthesis of chlorophyll *a* (Chl *a*) and light-harvesting complexes (Raven, 1990). SO phytoplankton have been shown, however, to employ a different strategy in dealing with low light availability by not increasing their Fe requirement, as they can enhance the size of their light-harvesting antennae instead of increasing the number of their Fe-rich photosystem units (Strzpek et al., 2012, 2019). This finding is supported by several studies reporting larger photosystem II (PSII) absorption cross-section (σ_{PSII}) of SO phytoplankton, especially under low light and Fe-depleted conditions (e.g., Ryan-Keogh et al., 2017; Alderkamp et al., 2019; Trimborn et al., 2019). While larger σ_{PSII} may be advantageous under low Fe and low light conditions, this may, however, be stressful when SO phytoplankton are exposed to high light intensities. Due to the larger antenna size, the efficiency of energy transfer from the light-harvesting complexes to the photosynthetic reaction centers may be reduced (Raven, 1990), thereby causing cellular stress. Indeed, previous shipboard incubation experiments have shown a higher susceptibility of SO phytoplankton to photoinhibition and decreased photosynthetic efficiency when cells are exposed to high light in conjunction with low Fe conditions (Alderkamp et al., 2010; Petrou et al., 2011). The susceptibility of Fe-limited SO phytoplankton to high light cannot be generalized because some field studies also reported that natural SO phytoplankton assemblages coped well with high irradiances even under Fe-limited conditions. For instance, in spring–summer field experiments in the Ross Sea, both the Fe-limited diatom- and *Phaeocystis*-dominated phytoplankton communities did not exhibit any photoinhibitory response even when exposed to high irradiances of up to 550 $\mu\text{mol photons m}^{-2} \text{s}^{-1}$ for over 6 days (Alderkamp et al., 2019). A similar capability to cope with high light stress (765 $\mu\text{mol photons m}^{-2} \text{s}^{-1}$) under low Fe supply was also reported for a subantarctic nanoflagellate-dominated phytoplankton community sampled during summer (Petrou et al., 2011). This could be attributed to the ability of Antarctic phytoplankton to photoacclimate such as by decreasing the concentration of its light-harvesting pigments (Van Leeuwe and Stefels, 1998; Luxem et al., 2017) and/or by releasing excess energy through non-photochemical quenching (NPQ; Falkowski and Raven, 2007).

The capability of SO phytoplankton to deal with varying light intensities greatly depends on their cellular Fe requirement, which has been reported to be species-specific. For example, a laboratory Fe–light incubation experiment by Trimborn et al. (2019) revealed that an Fe-limited flagellate *Phaeocystis antarctica* was able to maintain similar high growth rates irrespective of the light intensity, while another flagellate, the cryptophyte *Geminigera cryophila*, exhibited reduced carbon production at high light even when Fe supply was high (500 $\mu\text{mol photons m}^{-2} \text{s}^{-1}$; Camoying and Trimborn, 2023). In contrast, under low Fe supply, the Antarctic diatom *Chaetoceros debilis* was not able to grow at 500 $\mu\text{mol photons m}^{-2} \text{s}^{-1}$ (Trimborn et al., 2019). In line with the observations from these laboratory experiments, the spring *Phaeocystis*-dominated phytoplankton communities along the Western Antarctic Peninsula (WAP) also exhibited a strong positive response to light regardless of Fe availability (Joy-Warren et al., 2022). However, the summer diatom-dominated assemblage sampled in East Antarctica displayed the highest growth and biomass production only under Fe-replete conditions in combination with high light intensities (Vives et al., 2022). While there are already available studies that looked at the effects of Fe and light on diatom- and *Phaeocystis*-dominated natural SO assemblages, the response of communities dominated by other flagellates such as cryptophytes and dinoflagellates still remains less studied.

Climate change models project that net primary production in the SO would be enhanced as a whole due to a potential increase in Fe input and light availability in the future (Henley et al., 2020). Granted that this would be the case, it is crucial, however, to determine whether the magnitude of the projected increase in carbon production would be similar among SO phytoplankton assemblages dominated by different taxonomic groups. Hence, our study aims to address this knowledge gap by conducting field incubation experiments on the effects of Fe and light availability on the growth, carbon production, and photophysiology of two distinct natural Antarctic phytoplankton communities. Here, we compared the ecophysiological responses of the open ocean diatom-dominated assemblage and the coastal flagellate-dominated community to the increase in light and Fe supply.

Materials and methods

Field sampling and setup of two Fe–light shipboard phytoplankton incubation experiments

Two Fe–light shipboard bottle-incubation experiments were conducted during the *RV Polarstern* expedition PS97 (February–March 2016) to investigate the response of natural phytoplankton communities from two distinct environments in the Atlantic sector of the SO to increasing light and Fe availability. Both sampling locations, where the initial seawater was collected, had high macronutrients but different trace metal concentrations (Table 1). BIO 1, sampled on March 2, 2016, at 25-m depth in the Drake

TABLE 1 Initial conditions of BIO 1 and BIO 2 stations.

		BIO 1	BIO 2
Latitude	min ⁻¹	60° 24.78' S	60° 29.94' S
Longitude	min ⁻¹	66° 21.85' W	55° 29.70' W
dFe	nM	0.05	2.89
dMn	nM	0.15	1.00
dCu	nM	1.05	1.37
dZn	nM	3.21	11.11
dCo	nM	0.03	0.05
dFe:dMn	nM:nM	0.33	2.89
dFe:dCu	nM:nM	0.05	2.11
dFe:dZn	nM:nM	0.02	0.26
dFe:dCo	nM:nM	1.67	58
NO _x	μM	24	25
PO ₄	μM	1.50	1.49
SiOH ₄	μM	17	59
Chl <i>a</i>	μg L ⁻¹	0.05	1.04
LH: LP	ng ng ⁻¹	8.94	12.84

Coordinates, concentrations of total dissolved iron (dFe), dissolved manganese (dMn), dissolved copper (dCu), dissolved zinc (dZn), dissolved cobalt (dCo), macronutrients (NO_x = NO₃ (nitrate) and NO₂ (nitrite)), PO₄ = phosphate, SiOH₄ = silicate), chlorophyll *a* (Chl *a*) and ratios of light-harvesting (LH: sum of chlorophyll *a*, chlorophyll *c*₁₊₂, and fucoxanthin) to light-protective pigments (LP: sum of diadinoxanthin and diatoxanthin; LH:LP, ng ng⁻¹) are shown for the initial seawater sampled at BIO 1 and BIO 2 stations.

Passage (60° 24.78' S, 66° 21.85' W, 25 m), had very low concentrations of both total dissolved Fe (0.05 nM) and manganese (dMn; 0.15 nM), while station BIO 2, sampled on March 13, 2016, at 25-m depth and located close to the Antarctic Peninsula (60° 29.94' S, 55° 29.70' W, 25 m), had higher dFe (2.89 nM) and dMn (1.0 nM) values. Trace metal clean (TMC) techniques were employed for all seawater sampling of each incubation experiment according to the GEOTRACES guidelines (Cutter et al., 2017). Prior to the expedition, all bottles, tubing, and other labware were acid-cleaned in the laboratory, as previously described in Balaguer et al. (2022) and Pausch et al. (2022). At both stations, seawater was directly pumped into a clean container (US class 100, Opta, Bensheim, Germany) using a Teflon membrane pump (Almatec, Futur 50) and pre-filtered with a 200-μm mesh to remove mesozooplankton before filling the incubation bottles inside a laminar flow hood. Before sampling, the pump and tubing were flushed for at least 1 h with seawater at each location.

For the two shipboard incubation experiments, each natural phytoplankton community was exposed to three light levels—low light (LL; 30 μmol photons m⁻² s⁻¹), medium light (ML; 80 μmol photons m⁻² s⁻¹), and high light (HL; 150 μmol photons m⁻² s⁻¹)—in combination with *in situ* Fe concentrations (Control: no Fe addition) and after Fe addition (+Fe: addition of 0.9 nM FeCl₃). Light-emitting diode (LED) daylight lamps (SolarStinger LED Sun Strip Marine Daylight, Econlux, Cologne, Germany) were used as light sources and were set to the target light intensities. For each

light treatment, six incubation bottles (three Control and three +Fe) were aligned horizontally in front of the light source (Supplementary Figure 1). The incubation bottles were gently turned and shaken daily to prevent cells from settling at the bottom. To address potential “spatial effects” due to the arrangement of the bottles, their positions in front of the light source were also interchanged daily. Since the *in situ* concentrations of macronutrients were also high (Table 1), no additional macronutrient amendment was necessary. All treatments were conducted in triplicate TMC 2.5-L polycarbonate (PC) bottles and maintained under the above-described light intensities and a 16:8 (light:dark) hour cycle at 1°C simulating typical natural conditions of the sampling region and time. Depending on the Fe treatment, incubation experiments lasted 10–14 days. During the experiment, the photosynthetic efficiency of the community was monitored every 2–4 days after 1-h dark-acclimation via a Fast Repetition Rate Fluorometer [FRRf; Fast Ocean PTX sensor, Chelsea Technologies Group (CTG) Ltd., West Molesey, UK] at 1°C. At the start and end of each experiment, samples were collected to determine changes in phytoplankton community composition, photophysiology, elemental composition, and seawater chemistry.

Seawater chemistry

The concentration of the dissolved trace metals (TMs) (Fe, Mn, Cu, Zn, and Co) *in situ* was determined by filtering 100 mL of seawater through HCl-cleaned polycarbonate filters (0.2-μm pore size) using a TMC Nalgene filtration system. The filtrate was then collected into a PE bottle and stored triple-bagged at 2°C until analysis. As described in Balaguer et al. (2022), dTM concentrations were determined on a SeaFast system (Elemental Scientific, Omaha, NE, USA) (Hathorne et al., 2012; Rapp et al., 2017), coupled to an inductively coupled plasma–mass spectrometer (ICP-MS; Element2, resolution of R = 2000, Thermo Fisher Scientific, Waltham, MA, USA). An imino-diacetate (IDA) chelation column (part number CF-N-0200, Elemental Scientific) was used in the pre-concentration step. To minimize the adsorption of TMs onto the bottle walls and to reduce the formation of hydroxides during storage, the pre-filtered seawater samples were acidified to pH = 1.7 with a double-distilled nitric acid (HNO₃) and were UV-treated using a 450-W photo-chemical UV power supply (ACE GLASS Inc., Vineland, NJ, USA). Two blanks were taken during each digestion step, and daily optimization of the ICP-MS was performed to maintain oxide-forming rates below 0.3%.

Seawater samples were analyzed via external calibration to minimize any matrix effect, which could affect the quality of the analysis. The accuracy and precision of the method were assessed by analyzing a NASS-7 (National Research Council of Canada) reference standard in a 1:10 dilution (corresponding to environmentally representative concentrations) at the beginning and at the end of each run. All measured values were within the limits of the certified NASS-7 reference material with an average recovery rate of 97% for Fe, 91% for Mn, 98% for Cu, 94% for Zn, and 100% for Co.

Samples for the initial and final macronutrient concentrations for each experiment were filtered through a 0.2- μm filter and stored in a Falcon tube at -20°C . The concentration of dissolved macronutrients [total nitrate (nitrite + nitrate), phosphate, and silicate] was measured colorimetrically in the home laboratory on a QuAATro autoanalyzer (SEAL Analytical).

Pigments

Samples for photosynthetic pigment analyses were collected by filtering seawater onto 25-mm glass fiber filters (GF/F, Whatman). Filters were directly flash-frozen in liquid nitrogen and stored at -80°C . Concentrations of the pigments Chl *a*, chlorophyll *c1 + 2* (Chl *c1 + 2*), fucoxanthin, diadinoxanthin, alloxanthin, peridinin, and 19'-hexanoyloxyfucoxanthin were measured by high-performance liquid chromatography (HPLC). As described in detail in Pausch et al. (2022), pigments were extracted from the filters using acetone (>99.9% HPLC grade; Merck, Darmstadt, Germany), and the synthetic pigment canthaxanthin ($\geq 95\%$ HPLC grade, Sigma-Aldrich, St. Louis, MO, USA) was used as an internal standard. Pigment samples were analyzed using an HPLC system consisting of a Waters 600 controller (Waters Corporation, Milford, MA, USA) combined with a refrigerated autosampler (Waters 717 plus), a photodiode array detector (Waters 2996), and a fluorescence detector (Waters 2475). Pigments were then identified and quantified using the EMPOWER software (Waters). Specifically, pigments were identified by comparing their retention time to those of the standards, and concentrations were determined based on peak areas of external standards. Pigment concentrations were normalized to the extraction volume using the internal standard canthaxanthin. The ratio of light-harvesting (LH) pigments to light-protecting (LP) pigments was calculated by dividing the sum of the concentration of Chl *a*, Chl *c1+c2*, and fucoxanthin by the sum of the concentration of diadinoxanthin (DD) and diatoxanthin (DT) (Pausch et al., 2022).

Phytoplankton community composition

To determine the taxonomic composition of the natural phytoplankton community of both stations, unfiltered seawater samples were collected at the start and the end of the incubation experiments. For the BIO 1 experiment, samples were fixed with 1% (final v:v) Lugol's solution right after sampling and were allowed to settle in 10 mL Utermöhl sedimentation chambers (Hydro-Bios GmbH, Altenholz, Germany) for at least 24 h before counting them under an inverted microscope (Axio Observer D1, Carl Zeiss AG, Oberkochen, Germany). Phytoplankton were classified into four major groups of diatoms (*Fragilariopsis*, *Pseudo-nitzschia*, *Chaetoceros*, and other diatoms) and two flagellate groups (large, $>5 \mu\text{m}$; small, $<5 \mu\text{m}$). Cell growth rate (μ , d^{-1}) was calculated according to the following:

$$\mu = (\ln N_{T2} - \ln N_{T1}) / \Delta T$$

where N_{T1} and N_{T2} represent cell densities (cell mL^{-1}) at the start and the end of the experiment, respectively, and ΔT denotes the duration of the incubation (in days).

For the BIO 2 experiment, as it was not possible to identify the flagellates, which dominated the station, using microscopy, the phytoplankton community composition for this station was inferred from the HPLC pigment data. Specifically, the pigment fucoxanthin was used as a proxy for diatoms, peridinin for dinoflagellates, alloxanthin for cryptophytes, and 19'-hexanoyloxyfucoxanthin for haptophytes (Feng et al., 2010; Wright and Van den Enden, 2000; Mackey et al., 1996). Marker pigment to Chl *a* ratios were calculated for the initial community and at the end of the experiments to assess the percentage decrease or increase of the relative abundance of each phytoplankton group for the BIO 2 experiment. The following equation was used to calculate the change in the relative abundance (ΔRA , %) of target phytoplankton groups:

$$\Delta RA = [(PM: Chl a)_{T2} / (PM: Chl a)_{T1}] * 100$$

where (PM: Chl *a*)_{T1} and (PM: Chl *a*)_{T2} denote the ratio of specific pigment marker to Chl *a* at the start and end, respectively, of the BIO 2 incubation experiment.

Net particulate organic carbon production rates

For particulate organic carbon (POC) analysis, water was filtered for each replicate bottle onto pre-combusted (500°C, 15 h) 25-mm GF/F filters (Whatman). A filter blank was also taken as a blank sample for each bottle. All filters were placed in pre-combusted glass Petri dishes and were stored at -20°C . In the lab, filters were first dried at 50°C for >12 h and then acidified with 200 μL of 0.2 M HCl before samples were analyzed on an automated carbon nitrogen elemental analyzer (Euro EA-CN Elemental Analyzer, HEKAtech GmbH, Wegberg, Germany). Net daily POC production rates were calculated based on the difference between the initial and final POC concentrations over the duration of the incubation in days. To examine whether the phytoplankton assemblages of the two stations would increase their Fe demand with decreasing light (Fe-light antagonism; Sunda and Huntsman, 1997), the ratio of POC-based growth rate (μPOC) under Control ($\mu\text{POC}_{\text{Con}}$) to the μPOC under +Fe ($\mu\text{POC}_{+\text{Fe}}$) ($\mu\text{POC}_{\text{Con}} / \mu\text{POC}_{+\text{Fe}}$) was calculated for each light treatment. Based on Latour et al. (2023), the following equation was used to calculate the $\mu\text{POC}_{\text{Con}} / \mu\text{POC}_{+\text{Fe}}$ ratio:

$$\mu\text{POC}_{\text{Con}} / \mu\text{POC}_{+\text{Fe}} = \frac{\{[\ln(\text{POC}_{\text{Con}})_{T2} - \ln(\text{POC}_{\text{Con}})_{T1}] / \Delta T\}}{\{[\ln(\text{POC}_{+\text{Fe}})_{T2} - \ln(\text{POC}_{+\text{Fe}})_{T1}] / \Delta T\}}$$

where (POC_{Con}) and (POC_{+Fe}) represent the POC concentration ($\mu\text{mol L}^{-1}$) of the Control and +Fe treatments, respectively, at the start (T1) and the end (T2) of the experiment, and ΔT denotes the duration of the incubation (in days).

Photophysiology

An FRRf (FastOcean PTX sensor, CTG Ltd., West Molesey, UK) connected with a FastAct Laboratory system (CTG Ltd.) was used to measure Chl *a* fluorescence at the start, during, and end of the experiments of both stations. The fluorometer's LED had

excitation wavelengths of 450 nm, 530 nm, and 624 nm, and the light intensity was automatically adjusted. As in Balaguer et al. (2022) and Pausch et al. (2022), the single turnover mode was set with a saturation phase of 100 flashlets on a 2- μ s pitch followed by a relaxing phase of 40 flashlets on a 50- μ s pitch. In order to allow full oxidation of all PSII reaction centers, samples were dark-acclimated for 1 h before each measurement. The minimum (F_0) and maximum (F_m) Chl *a* fluorescence of PSII were measured six times with the use of the FastPro8 software (Version 1.0.55, Kevin Oxborough, CTG Ltd.). The maximum quantum yield of photochemistry in PSII (F_v/F_m , rel. unit) was then calculated using the following equation:

$$F_v/F_m = (F_m - F_0)/F_m$$

Using the single turnover measurements of the dark-acclimated community, the functional absorption cross-section of PSII (σ_{PSII} , nm² PSII⁻¹), the time constant for electron transport at the acceptor side of PSII (τ_{Qa} , μ s), and the connectivity factor (P , dimensionless) were derived as in Oxborough et al. (2012). Electron transport rate (ETR)–irradiance curves were performed, and the ETRs (e⁻ PSII⁻¹ s⁻¹) were calculated using the following formula (Suggett et al., 2004, 2009; Huot and Babin, 2010; Schuback et al., 2015):

$$ETR = \sigma_{PSII} * ((F'_q/F'_m) / (F_v/F_m)) * E$$

where (F'_q/F'_m) denotes the effective PSII quantum yield under ambient light and E is the irradiance level (photons m⁻² s⁻¹). The maximum ETR (ETR_{max}, e⁻ PSII⁻¹ s⁻¹), maximum light utilization efficiency (α , rel. unit), and minimum saturation irradiance (I_k , μ mol photons m⁻² s⁻¹) were calculated from the ETR–irradiance curve based on Ralph and Gademann (2005). The Stern–Volmer equation was used to calculate the NPQ:

$$NPQ = F_m/F'_m - 1$$

Statistics

Two-way analysis of variance (ANOVA) with Tukey's multiple comparison *post-hoc* tests was used to statistically analyze the interactive effects of the two Fe (Control and +Fe) and three light (LL, ML, and HL) treatments on all experimental parameters. Due to the nature of the light source used in the experiments as well as the specific spatial arrangement of the incubation bottles, any test of light effects is a test of both light and spatial effects. All statistical analyses were performed using the program GraphPad Prism (Version 10.1.0 (316) for Windows, GraphPad Software, San Diego, CA, USA), and the significance testing was conducted at the $p < 0.05$ level.

Results

Initial chemical and biological characteristics of both sampling stations

Shipboard Fe–light incubation experiments were conducted with phytoplankton communities sampled in two distinct environments.

The phytoplankton community collected at station BIO 1 was located in the open waters of the Drake Passage. Here, macronutrient concentrations were high (Table 1), while only low levels of chlorophyll *a* (Chl *a*) and the trace metals Fe and Mn were found (Table 1). The initial phytoplankton community of BIO 1 also exhibited very low photosynthetic efficiency (F_v/F_m) together with large functional absorption cross-sections of PSII (σ_{PSII}) (Table 2). The initial micro-phytoplankton community of station BIO 1 was dominated by diatoms composed mainly of the genera *Fragilariopsis*, *Chaetoceros*, and *Pseudo-nitzschia*, while the nanoflagellate group was present only in smaller numbers. Based on Balaguer et al. (2022), the most abundant phytoplankton group *Fragilariopsis* was FeMn-co-limited, while the other phytoplankton groups (*Chaetoceros*, *Pseudo-nitzschia*, and *Phaeocystis*) were only Fe-limited. The initial BIO 1 phytoplankton community was also found to be light-limited based on the observations of Pausch et al. (2022).

In contrast, the BIO 2 station was located close to the WAP and had way higher concentrations of dFe (2.89 nM) and dMn (1.0 nM) than BIO 1 (Table 1). In line with this, F_v/F_m (0.38 ± 0.01) and Chl *a* (1.04μ g L⁻¹) values of the initial community of the BIO 2 station were also much higher compared to the initial community of BIO 1. Based on Blanco-Ameijeiras et al. (2020), the BIO 2 phytoplankton community was dominated by flagellates represented by prymnesiophytes, choanoflagellates, dinoflagellates, and cryptophytes, while diatoms were observed only in low concentrations. The authors also reported that the BIO 2 initial assemblage was only mildly Fe-limited.

BIO 1: POC production, phytoplankton community structure, and photoacclimation

At the end of the experiment (Control, 11-day duration; +Fe, 10-day duration), POC production of the phytoplankton community sampled in BIO 1 was significantly influenced by Fe ($p < 0.0001$) and light alone ($p < 0.0001$) as well as their interaction ($p < 0.0043$) (Figure 1A; Table 3). Fe addition significantly increased POC production rates in all light treatments (Figure 1). For the Control treatments, POC production increased with increasing light intensity. In the +Fe treatments, POC production was strongly stimulated between LL and ML, while no further stimulation was observed between ML and HL (Figure 1). Looking at the POC-based growth rates (μ POC) of the BIO 1 assemblage, the ratio of μ POC in the Control (μ POC_{Con}) to μ POC in the +Fe (μ POC_{+Fe}) was similar between LL and ML and increased at HL (μ POC_{Con}/ μ POC_{+Fe}; Table 4).

Growth rates of each counted phytoplankton group (Figure 2) were significantly influenced by both Fe (diatoms and nano- and small flagellates, $p < 0.0001$; big flagellates, $p = 0.0224$) and light (diatoms and nano- and small flagellates, $p < 0.000$; big flagellates, $p = 0.0006$) alone, but no interactive effects between the two factors were observed (Table 3). Irrespective of the light level, Fe enrichment enhanced the growth of all phytoplankton groups except for the large-sized flagellates, for which a significant increase in growth was observed only at ML. In response to

TABLE 2 The dark-adapted maximum photosystem II quantum yield (F_v/F_m), the functional absorption cross-section of PSII (σ_{PSII}), energy transfer between photosystem II units (connectivity, P), re-oxidation times of the primary electron acceptor Qa (τ_{QA}), maximum electron transport rates (ETR_{max}), minimum saturating irradiance (I_k), and the maximum light utilization efficiency (α) of the natural phytoplankton communities sampled in BIO 1 and BIO 2 stations after growing them at low light (LL; 30 $\mu\text{mol photons m}^{-2} \text{s}^{-1}$), middle light (ML; 80 $\mu\text{mol photons m}^{-2} \text{s}^{-1}$), and high light (HL; 150 $\mu\text{mol photons m}^{-2} \text{s}^{-1}$) under *in situ* iron concentrations (Con) and after Fe addition (+Fe) conditions.

Station	Fe	Light	F_v/F_m (dimensionless)	σ_{PSII} ($\text{nm}^2 \text{PSII}^{-1}$)	P (dimensionless)	τ_{QA} (μs)	ETR_{max} ($\text{e}^- \text{PSII}^{-1} \text{s}^{-1}$)	I_k ($\mu\text{mol photons m}^{-2} \text{s}^{-1}$)	α (rel. unit)
BIO 1 initial			0.16 ± 0.03	5.3 ± 0.37	0.23 ± 0.03	619 ± 76	408	118	3.45
BIO 1	Con	LL	0.34 ± 0.07^a	3.2 ± 0.5^a	0.34 ± 0.03^{ac}	603 ± 49^a	159 ± 18^a	87 ± 18^a	1.84 ± 0.17^a
Bio 1	Con	ML	0.24 ± 0.06^a	3.8 ± 0.5^a	0.22 ± 0.07^b	502 ± 65^b	334 ± 57^{ab}	166 ± 25^b	2.02 ± 0.21^a
Bio 1	Con	HL	0.30 ± 0.06^a	3.7 ± 1.4^a	0.28 ± 0.07^{ab}	590 ± 30^a	404 ± 206^b	220 ± 46^c	1.76 ± 0.52^a
Bio 1	+Fe	LL	0.43 ± 0.01^b	2.5 ± 0.08^{ab}	0.41 ± 0.01^c	610 ± 19^{ac}	134 ± 4^{ac}	70 ± 6^a	1.93 ± 0.14^a
Bio 1	+Fe	ML	0.34 ± 0.02^b	2.7 ± 0.19^{ab}	0.33 ± 0.01^{ac}	574 ± 18^c	177 ± 8^c	105 ± 5^a	1.68 ± 0.06^a
Bio 1	+Fe	HL	0.34 ± 0.05^{ab}	2.5 ± 0.15^b	0.28 ± 0.01^a	586 ± 17^{bc}	184 ± 19^{ac}	118 ± 15^a	1.56 ± 0.06^a
BIO 2 initial			0.38 ± 0.01	6.0 ± 0.26	0.39 ± 0.01	679 ± 35	221	144	1.53
BIO 2	Con	LL	0.31 ± 0.00^a	3.0 ± 0.63^{ab}	0.23 ± 0.04^a	644 ± 42^a	91 ± 18^a	61 ± 3^a	1.50 ± 0.38^a
Bio 2	Con	ML	0.31 ± 0.00^a	3.5 ± 0.06^a	0.22 ± 0.03^a	603 ± 20^a	186 ± 13^b	106 ± 7^b	1.76 ± 0.06^a
Bio 2	Con	HL	0.30 ± 0.01^a	2.6 ± 0.25^b	0.20 ± 0.01^a	613 ± 28^a	146 ± 6^c	102 ± 10^b	1.44 ± 0.13^a
Bio 2	+Fe	LL	0.40 ± 0.01^b	2.3 ± 0.12^c	0.35 ± 0.04^b	660 ± 23^{ab}	89 ± 6^a	59 ± 3^a	1.51 ± 0.04^a
Bio 2	+Fe	ML	0.38 ± 0.05^b	3.3 ± 0.24^a	0.29 ± 0.06^b	611 ± 23^{ab}	197 ± 15^b	127 ± 13^c	1.56 ± 0.09^a
Bio 2	+Fe	HL	0.38 ± 0.00^b	2.2 ± 0.05^{bc}	0.31 ± 0.03^b	661 ± 8^b	124 ± 8^d	97 ± 9^b	1.29 ± 0.06^a

Values represent the means (\pm SD) of triplicate incubations. Significant differences between treatments are indicated by varying lowercase letters (*post-hoc* tests, $p < 0.05$).

increasing light under Control conditions, the growth of *Fragilariopsis* was stimulated, while that of all other phytoplankton groups remained the same between LL and ML and increased only at HL. In response to increasing light under +Fe conditions, the growth of most groups was stimulated but depended on the applied light intensity. For instance, the growth of *Chaetoceros* was stimulated across all light levels, while the growth of *Pseudo-nitzschia*, *Fragilariopsis*, and the large-sized flagellates increased only from LL to ML with no further change at HL. In comparison, the growth of the other diatoms and the small flagellates was enhanced only between ML and HL (Figure 2).

At the end of the experiment, the ratio of LH to light-protective pigments (LP; LH: LP, ng ng^{-1}) of the BIO 1 phytoplankton community was influenced by both light ($p < 0.0001$) and Fe ($p < 0.0001$) alone, but not by their interaction (Table 3). An Fe-dependent stimulation of LH: LP ratios was observed in all light treatments (Figure 3). Irrespective of Fe availability, the LH: LP ratio decreased from LL to ML and remained unchanged toward HL (Figure 3).

The F_v/F_m and the connectivity between adjacent photosystems (P) were influenced by both Fe (F_v/F_m , $p = 0.0053$; P , $p = 0.0102$) and light (F_v/F_m , $p = 0.0137$; P , $p = 0.0024$) alone. Fe addition led to higher F_v/F_m values except at HL. In response to increasing irradiance, F_v/F_m remained the same regardless of Fe availability (Table 2). P generally increased with Fe addition, but the change was significant only at ML. Irrespective of Fe availability, P decreased from LL to ML and remained the same at HL. The functional absorption cross-sections of PSII (σ_{PSII}) were influenced only by Fe ($p = 0.0057$) whereby a decrease was observed in the HL and +Fe treatments. The time constant for electron

transfer at PSII (τ_{QA}) responded to light alone ($p = 0.0239$), decreasing from LL to ML and increasing again between ML and HL in the Control (Table 2). No interactive effect of Fe and light on all photophysiological parameters (F_v/F_m , σ_{PSII} , P , and τ_{QA}) of the phytoplankton assemblage in BIO 1 was observed (Table 3).

The maximum electron transport rates (ETR_{max}) and minimum saturating irradiances (I_k) of the BIO 1 phytoplankton assemblage were influenced by both Fe (ETR_{max} , $p = 0.0071$; I_k , $p = 0.0002$) and light alone (ETR_{max} , $p = 0.0343$; I_k , $p < 0.0001$), while a significant interactive Fe–light effect ($p = 0.0283$) was evident only for I_k (Table 3). Fe addition resulted in lower ETR_{max} and I_k values, but this effect was only significant for ML and HL. Increasing irradiance led to higher ETR_{max} for ML compared to LL but not HL, and I_k values, but only in the Control treatment (Table 2; Figures 4A, B). The maximum light utilization efficiency (α), however, was affected by neither light nor Fe (Table 2). NPQ values of the final communities in BIO 1 were enhanced with increasing irradiance during the fluorescence light curve (FLC) in all treatments (Figure 5A). While lower NPQ values were observed in +Fe compared to the Control treatments, light availability in all cases did not have an influence on NPQ.

BIO 2: POC production, phytoplankton community structure, and photoacclimation

For the BIO 2 station, at the end of the experiment (Control: 14-day duration; +Fe: 11-day duration), POC production was positively

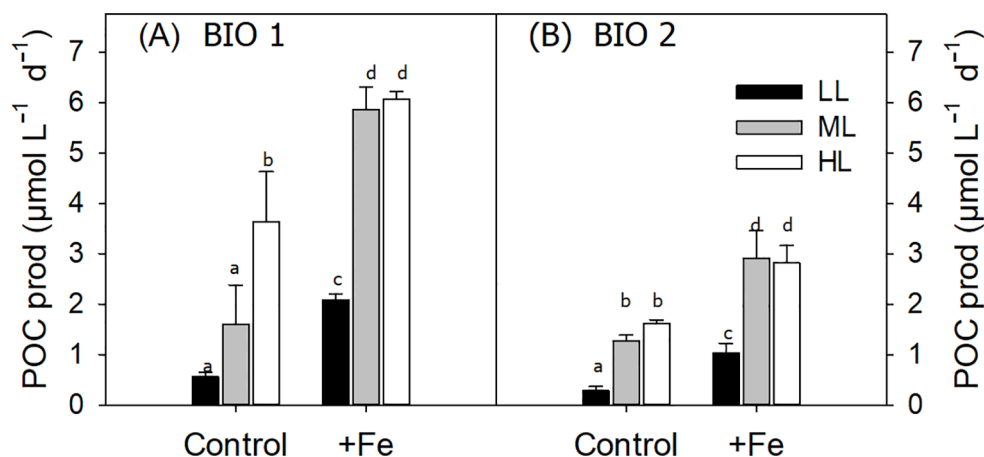


FIGURE 1

Daily particulate organic carbon (POC) production rates of the phytoplankton communities sampled at stations BIO 1 (A) and BIO 2 (B) after growing them at low light (LL; $30 \mu\text{mol photons m}^{-2} \text{ s}^{-1}$), middle light (ML; $80 \mu\text{mol photons m}^{-2} \text{ s}^{-1}$), and high light (HL; $150 \mu\text{mol photons m}^{-2} \text{ s}^{-1}$) in conjunction with *in situ* iron concentrations (Control) or after iron addition (+Fe). Values represent the means (\pm SD) of triplicate incubations. Significant differences between treatments are indicated by varying lowercase letters (*post-hoc* tests, $p < 0.05$).

influenced by both Fe ($p < 0.0001$) and light ($p < 0.0001$) alone, but not their interaction (Table 3). In response to Fe addition, POC production increased significantly in all light treatments. Irrespective of Fe availability, increasing light intensity stimulated POC production rates between LL and ML, while values remained unchanged between ML and HL (Figure 1B). The $\mu\text{POC}_{\text{Con}}/\mu\text{POC}_{+\text{Fe}}$ ratios increased from LL to ML and remained the same at HL (Table 4).

Since it was not feasible to count the flagellate groups using microscopy for the BIO 2 samples, the ratio of pigment marker to Chl *a* was used instead as a proxy to assess the relative changes of the major phytoplankton taxa [fucoxanthin (Fuco): diatoms; peridinin (Peri): dinoflagellates; alloxanthin (Allo): cryptophytes; 19'-hexanoxyfucoxanthin (19'-hexa): haptophytes] over the course of the BIO 2 experiment (Figure 6). In all incubation bottles, among the four taxa, only the haptophyte group exhibited an overall decrease ($\sim 60\%$) in its abundance relative to their number at the start of the experiment. In contrast, at the end of the incubation, the relative abundance of diatoms either remained unchanged or increased slightly, while dinoflagellates and cryptophytes exhibited up to a twofold increase in abundance depending on the treatment. In all light treatments, Fe addition had no effect on the relative abundance of the cryptophytes and haptophytes, while a decrease in diatoms was observed at LL, and there was higher dinoflagellate abundance in both the LL and ML treatments in +Fe compared to Control. In response to increasing light intensity, diatom abundance represented by Fuco concentrations did not change except under the Control treatment where their relative abundance decreased from LL to ML. Dinoflagellate abundance was only influenced by light under the +Fe treatment, being decreased from ML to HL. In both the Control and +Fe treatments, the abundance of cryptophytes was enhanced at HL relative to LL. However, increasing light only had a

positive effect on the abundance of haptophytes under the Control, while values remained unchanged in the +Fe (Figure 6).

Fe addition did not have any effect on the LH: LP ratios. Increasing light, however, negatively influenced LH: LP ratios ($p < 0.0001$) except when Fe was added, and the ratio remained the same between ML and HL (Figure 3B). In general, the F_v/F_m and P values of the final BIO 2 phytoplankton assemblage were influenced only by Fe alone ($p < 0.0001$), while light and the combination of both factors had no effect. Accordingly, only the addition of Fe significantly increased F_v/F_m and P in all light treatments (Table 2). Both single Fe ($p = 0.0054$) and light ($p = 0.0003$) effects were observed in σ_{PSII} (Table 3). Fe addition decreased σ_{PSII} only at LL. In the Control, increasing irradiance resulted in similar σ_{PSII} between LL and ML but was decreased at HL, while in the +Fe, σ_{PSII} was enhanced from LL to ML and decreased at HL. τ_{QA} was affected by neither light nor Fe except at HL where it was significantly increased after Fe addition (Table 2).

Fe addition did not influence ETR_{max} of LL and ML treatments but significantly reduced ETR_{max} of the HL treatment (Table 2). Increasing light intensity led to an increase in ETR_{max} values ($p < 0.0001$) in all treatments (Figures 4C, D). I_k remained unchanged with Fe addition except in the ML, which exhibited higher I_k values. I_k was altered in response to increasing irradiance ($p < 0.0001$) but differently affected depending on the Fe availability. Both the Control and +Fe treatments exhibited an increase in I_k from LL to ML, but in the Control, I_k did not change between ML and HL, while it was reduced from ML to HL in the +Fe. Neither light nor Fe had an influence on α of the phytoplankton communities in BIO 2 (Table 2). In all treatments, NPQ values were enhanced with increasing actinic irradiance during the fluorescence light curve runs but unaffected by Fe availability. Interestingly, the Control ML had the highest NPQ values in response to varying light, while values were relatively similar among the three light treatments under +Fe (Figures 5C, D).

TABLE 3 Significance of the single effects of light and Fe as well as their interactive effects effects on the different physiological parameters.

Parameter	Light	Fe	Interaction
BIO 1			
POC production	<0.0001	<0.0001	0.0043
<i>Fragilariopsis</i> , μ	<0.0001	<0.0001	No
<i>Pseudo-nitzschia</i> , μ	<0.0001	<0.0001	No
<i>Chaetoceros</i> , μ	<0.0001	<0.0001	No
Other diatoms, μ	<0.0001	<0.0001	No
Nanoflagellates, μ	<0.0001	<0.0001	No
Big flagellates, μ	0.0006	0.0224	No
Small flagellates, μ	<0.0001	<0.0001	No
LH: LP ratio	<0.0001	<0.0001	No
F_v/F_m	0.0137	0.0053	No
σ_{PSII}	No	0.0057	No
P	0.0024	0.0102	No
τ_{Qa}	0.0239	No	No
ETR_{max}	0.0343	0.0071	No
I_k	<0.0001	0.0002	0.0283
α	No	No	No
BIO 2			
POC production	<0.0001	<0.0001	No
LH: LP ratio	<0.0001	No	No
F_v/F_m	No	<0.0001	No
σ_{PSII}	0.0003	0.0054	No
P	No	0.0001	No
τ_{Qa}	0.0310	No	No
ETR_{max}	<0.0001	No	No
I_k	<0.0001	No	0.0366
α	0.0369	No	No
Fucoxanthin	No	0.0140	No
Peridinin	0.0213	0.0310	0.0142
Alloxanthin	0.0039	0.0135	No
19'-Hexanoyloxyfucoxanthin	0.0253	No	No

Discussion

Our study shows that both Fe addition and increasing light stimulated the POC production of the two phytoplankton communities. The degree of POC production increase, however, varied between the two wherein it was slightly higher in the diatom-dominated BIO 1 assemblage compared to the flagellate-dominated BIO 2 community. This differential response to Fe could be attributed to the species-specific cellular Fe demand and the Fe uptake

capabilities of the dominant phytoplankton groups in each station. While SO phytoplankton commonly increase their σ_{PSII} under Fe limitation, we did not observe such physiological adjustment in most of our treatments. Accordingly, both communities increased their Fe demand with decreasing light availability. We also show here that POC production was not enhanced further between ML and HL even when Fe was added, potentially indicating that both communities had additional requirements, which were not fulfilled (e.g., availability of other trace metals such as Mn).

Fe addition stimulated the POC production of the phytoplankton community at both stations and in all light treatments

In line with the observations of previous studies with SO natural phytoplankton assemblages (e.g., Feng et al., 2010; Alderkamp et al., 2015; Balaguer et al., 2022; Joy-Warren et al., 2022; Pausch et al., 2022; Vives et al., 2022) and laboratory cultures (e.g., Andrew et al., 2019; Koch et al., 2019; Koch and Trimborn, 2019; Camoying et al., 2022), POC production rates of both stations were stimulated after Fe addition relative to the Control, indicating Fe limitation of both communities. However, the degree of the limitation differed between the two stations (Figure 1). The diatom-dominated BIO 1 station had a very low dFe concentration and a low F_v/F_m value *in situ*; hence, Fe addition resulted in a 100% increase of F_v/F_m values in the +Fe treatments relative to the initial. In addition, σ_{PSII} values of the +Fe treatments were reduced by 50% after Fe addition compared to the initial value (Table 2). However, different from the observations of other studies showing a decrease in σ_{PSI} in response to Fe enrichment (Petrou et al., 2014; Strzepak et al., 2019), we only observed an Fe-dependent decrease in σ_{PSI} at HL (Table 2). Similarly, the initial LH:LP ratio of BIO 1 was also low, with Fe amendment leading to much higher LH:LP ratios in the +Fe treatments (Figure 3). As Fe is required in chlorophyll synthesis, it is a common response of SO phytoplankton to increase the concentration of light-harvesting pigments after Fe enrichment (Van Leeuwe and Stefels, 1998; Moore et al., 2007; Alderkamp et al., 2012). The above observations indicate that the *in situ* BIO 1 community was severely Fe-limited, in line with the findings of Blanco-Ameijeiras et al. (2020) and Pausch et al. (2022). By contrast, the flagellate-dominated BIO 2 station had a high dFe concentration together with a high F_v/F_m value *in situ*. This is similar to observations for the BIO 2 community by Blanco-Ameijeiras et al. (2020), who also demonstrated in their Fe addition experiments that the BIO 2 community was mildly Fe-limited. Based on our data, the BIO 2 flagellate-dominated community exhibited lower F_v/F_m values in all of its Control treatments compared to the initial (Table 2). It could be that Fe was depleted over the incubation period due to the high cellular Fe requirement of flagellates. In line with this, open ocean nanophytoplankton was found to acquire both new and recycled Fe compared to large-sized diatoms, which are not able to utilize the latter (Boyd et al., 2012). Moreover, Twining et al. (2004) reported higher Fe:C ratios in SO flagellates than diatoms, suggesting a higher Fe demand of the former in sustaining growth as has been observed for the cryptophyte *G. cryophila* (Camoying et al., 2022).

TABLE 4 Particulate organic carbon-based growth rates (μPOC , d^{-1}) of the natural phytoplankton communities sampled in BIO 1 and BIO 2 stations after growing them at low light (LL; $30 \mu\text{mol photons m}^{-2} \text{s}^{-1}$), middle light (ML; $80 \mu\text{mol photons m}^{-2} \text{s}^{-1}$), and high light (HL; $150 \mu\text{mol photons m}^{-2} \text{s}^{-1}$) under *in situ* iron concentrations (Con) and after Fe addition (+Fe) conditions.

Station	POC-based growth rate (μPOC , d^{-1})						$\mu\text{POC}_{\text{Con}}/\mu\text{POC}_{+\text{Fe}}$		
	LL		ML		HL		LL	ML	HL
	$\mu\text{POC}_{\text{Con}}$	$\mu\text{POC}_{+\text{Fe}}$	$\mu\text{POC}_{\text{Con}}$	$\mu\text{POC}_{+\text{Fe}}$	$\mu\text{POC}_{\text{Con}}$	$\mu\text{POC}_{+\text{Fe}}$			
BIO 1	0.08 ± 0.01	0.18 ± 0.00	0.12 ± 0.01	0.27 ± 0.01	0.21 ± 0.02	0.27 ± 0.00	0.45 ± 0.07^a	0.47 ± 0.05^a	0.77 ± 0.07^b
BIO 2	0.03 ± 0.01	0.07 ± 0.01	0.08 ± 0.00	0.14 ± 0.01	0.09 ± 0.00	0.13 ± 0.01	0.35 ± 0.09^a	0.57 ± 0.06^b	0.67 ± 0.05^b

Values represent the means (\pm SD) of triplicate incubations. Significant differences between light treatments are indicated by varying lowercase letters (*post-hoc* tests, $p < 0.05$).

The distinct phytoplankton community composition of each station and their differential Fe uptake capabilities as well as Fe demand most likely influenced the overall POC production in BIO 1 and BIO 2. The degree of Fe-dependent increase in POC production varied between the two stations, being slightly higher in BIO 1 than in BIO 2. In BIO 1, POC production in the +Fe was on average two times higher than in the Control, while it was only 1.6 times higher in BIO 2. In line with this, growth rates of all phytoplankton groups in BIO 1 were also strongly promoted after Fe addition (Figure 2), while Fe enrichment, except for the dinoflagellate group, had no effect on the relative abundances of the other phytoplankton groups in BIO 2 (Figure 6). The high resource uptake capabilities of diatoms as *r* strategists (Arrigo et al., 2005) as well as their low Fe demand (Sunda et al., 1991; Marchetti et al., 2006) could be the reason for the sustained dominance of diatoms over flagellates in BIO 1, being, therefore, the primary drivers of enhanced POC production at this station. However, the higher Fe requirement of flagellates (high Fe:C ratios; Twining et al., 2004; Camoying et al., 2022) could be responsible for the smaller degree of increase in POC production of the BIO 2 community and the absence of positive Fe effects on the growth of almost all BIO 2 phytoplankton groups, despite the high *in situ* dFe concentration.

BIO 1: The Fe-enriched BIO 1 community required medium irradiance to yield highest POC production rates

Even though increasing light enhanced the overall growth of the Fe-enriched BIO 1 assemblage, similar photophysiological characteristics were maintained between light treatments (Table 2), indicating optimal photoacclimation of the diatom-dominated communities. The growth of various phytoplankton groups was, however, differentially affected by increasing light levels (Figure 2). *Fragilariopsis*, *Chaetoceros*, *Pseudo-nitzschia*, and the large-sized flagellates, among them *P. antarctica*, increased their growth rates from LL to ML. Similar light-dependent stimulation in the growth of Fe-replete *Fragilariopsis* was already previously observed for *Fragilariopsis curta* (Heiden et al., 2016), *Fragilariopsis cylindrus* (Ye et al., 2023), and *Fragilariopsis pseudonana* (Heiden et al., 2019). As in this study, previous studies have reported a positive effect of increasing light on the

growth of *Chaetoceros lineola* (Feng et al., 2010), *C. debilis* (Trimborn et al., 2019), and *Pseudo-nitzschia prolongatoides/subcurvata* (Lee et al., 2022) as well as the flagellate *P. antarctica* (Feng et al., 2010; Strzepak et al., 2012; Lee et al., 2022). From ML to HL, *Chaetoceros* showed even further light-dependent growth stimulation, as previously observed in other studies (Feng et al., 2010; Trimborn et al., 2019). In addition to *Chaetoceros*, the other diatoms and small-sized flagellates also exhibited the highest growth rates at HL. This suggests that Fe addition allowed them to take advantage of the HL availability. Based on our results, the growth of the BIO 1 community was clearly limited by Fe and light.

As observed in other field studies with natural SO phytoplankton communities (Viljoen et al., 2018; Alderkamp et al., 2019; Joy-Warren et al., 2022; Latour et al., 2023), the increasing light intensity from LL to ML promoted a strong enhancement in POC production (181%) of the Fe-enriched BIO 1 community (Figure 1A). However, no further increase in POC production was observed from ML to HL in spite of the increase in growth of *Chaetoceros*, the other diatoms, and the small flagellate group at HL. This suggests that these three groups were not the main drivers of POC production at HL in BIO 1, but instead, production rates were more strongly influenced by *Fragilariopsis*, which dominated the initial BIO 1 community. In fact, in the +Fe treatment, the growth of *Fragilariopsis* was enhanced between LL and ML but remained the same at HL. *Fragilariopsis* of the BIO 1 community was identified to suffer from FeMn-co-limitation *in situ*, as it yielded the highest growth rates only when both Fe and Mn were supplied (Balaguer et al., 2022). Since Mn is a crucial component of the PSII water-splitting center (Raven, 1990), it could be that the HL conditions in our study triggered a higher Mn demand for *Fragilariopsis*, which was, however, not fulfilled, as only Fe was supplied in this study, preventing thus its growth stimulation from ML to HL under high Fe conditions. Indeed, an increased Mn demand under HL conditions ($>120 \mu\text{mol photons m}^{-2} \text{s}^{-1}$ PAR; Joy-Warren et al., 2022) was reported for the springtime phytoplankton community from the WAP region of the SO. It could also be that due to the unfulfilled high Mn demand of *Fragilariopsis*, the HL exposure led potentially to higher oxidative stress. The cells may have prioritized the allocation of the available Fe for the production of Fe superoxide dismutase (FeSOD) to reduce the formation of reactive oxygen species (ROS) (Peers and Price, 2004). Hence, as a consequence, no further increase in carbon production was observed between ML and HL treatments of the BIO 1 community under high Fe supply.

BIO 1: The Fe-limited BIO 1 community required high light to achieve maximum POC production

Comparing the F_v/F_m and LH:LP ratios of the Control LL to those of the initial community, it can be seen that both parameters increased at the end of the incubation (Table 2; Figure 3). This indicates the relief of light limitation and photoacclimation of the Fe-limited community to a constant and stable light supply over the course of the

experiments. In line with the observations of other studies (Vives et al., 2022; Alderkamp et al., 2019; Viljoen et al., 2018), the exposure of the BIO 1 Control community to increasing light levels did not alter F_v/F_m and σ_{PSII} (Table 2). While previous studies have found that HL conditions ($>300 \mu\text{mol photons m}^{-2} \text{s}^{-1}$) can induce additional light stress in Fe-limited phytoplankton (Moore et al., 2007; Alderkamp et al., 2010, 2019), this was not the case here, probably due to the fact that the applied HL treatment of $150 \mu\text{E}$ was not high enough. As in Petrou et al. (2011), LH:LP ratios (Figure 3A) and the connectivity

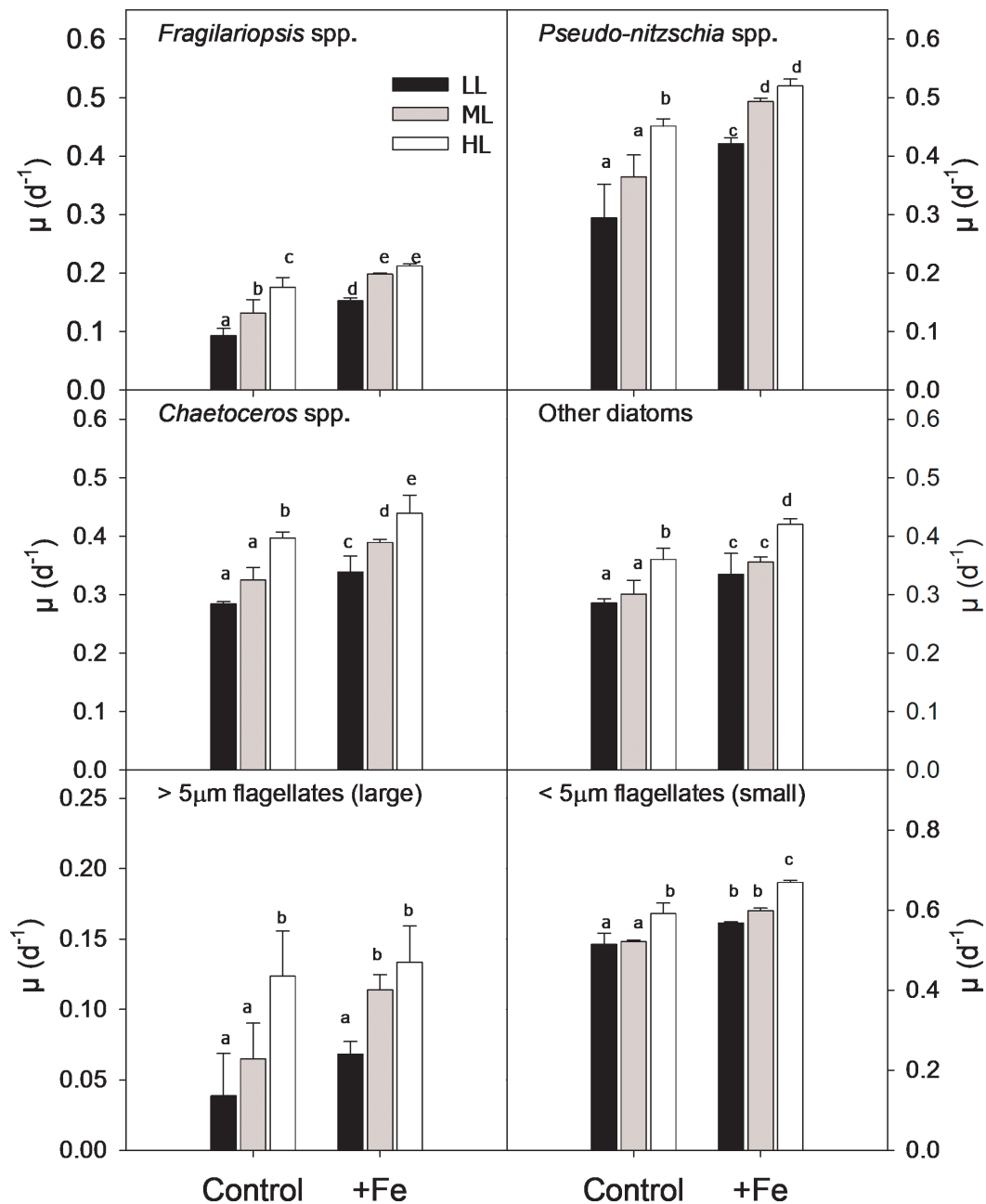


FIGURE 2 Growth rates of the different phytoplankton groups [*Fragilariopsis* spp. (A), *Pseudo-nitzschia* spp. (B), *Chaetoceros* spp. (C), other diatoms (D), large flagellates (E), and small flagellates (F)] from BIO 1 station after growing at low light (LL; $30 \mu\text{mol photons m}^{-2} \text{s}^{-1}$), middle light (ML; $80 \mu\text{mol photons m}^{-2} \text{s}^{-1}$), and high light (HL; $150 \mu\text{mol photons m}^{-2} \text{s}^{-1}$) in conjunction with *in situ* iron concentrations (Control) and after iron addition (+Fe). Values represent the means (\pm SD) of triplicate incubations. Significant differences between treatments are indicated by varying lowercase letters (*post-hoc* tests, $p < 0.05$).

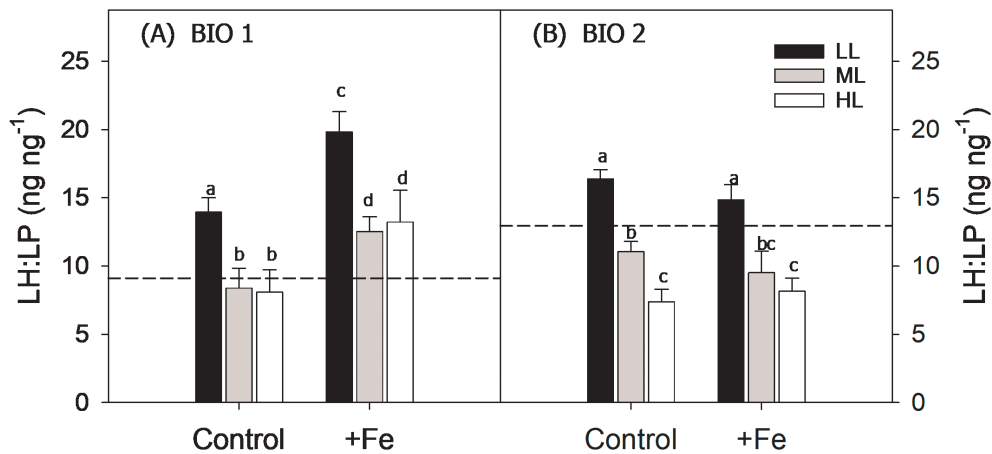


FIGURE 3

Ratios of light-harvesting (LH; sum of chlorophyll *a*, chlorophyll *c*_{1 + 2}, and fucoxanthin) to light-protective pigments (LP; sum of diadinoxanthin and diatoxanthin; LH: LP, ng ng^{-1}) of the phytoplankton communities sampled in BIO 1 (A) and BIO 2 (B) stations after growing them at low light (LL; 30 $\mu\text{mol photons m}^{-2} \text{s}^{-1}$), middle light (ML; 80 $\mu\text{mol photons m}^{-2} \text{s}^{-1}$), and high light (HL; 150 $\mu\text{mol photons m}^{-2} \text{s}^{-1}$) in conjunction with *in situ* iron concentrations (Control) and after iron addition (+Fe). The initial LH: LP ratios of the starting communities of each station are presented as black dashed lines. Values represent the means (\pm SD) of triplicate incubations. Significant differences between treatments are indicated by varying lowercase letters (*post-hoc* tests, $p < 0.05$).

between photosystems (*P*; Table 2) were reduced between LL and ML, indicating active photoacclimation to absorb less light under ML by the Fe-limited BIO 1 community. As a consequence, I_k significantly increased between LL and ML (Table 2), indicating that more light

was required to saturate photosynthesis. In fact, the re-oxidation time of Qa (τ_{QA}) was much shorter (Table 2), yet this did not translate into more efficient electron cycling (Table 2) and POC production (Figure 1A), suggesting that the Calvin cycle was not saturated.

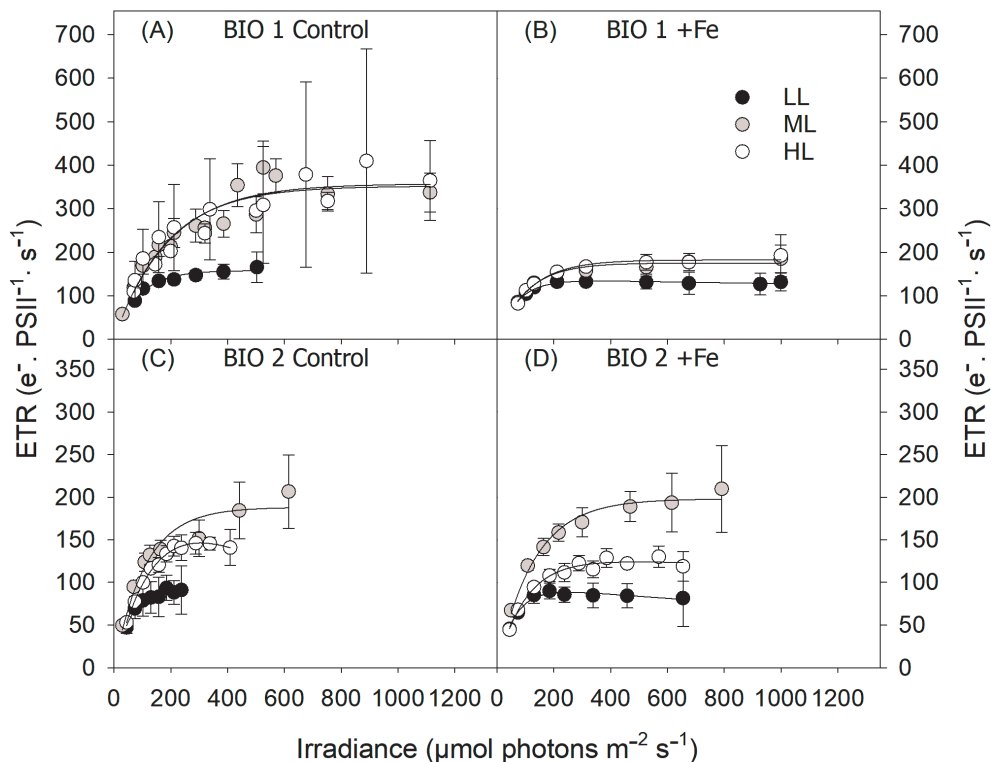
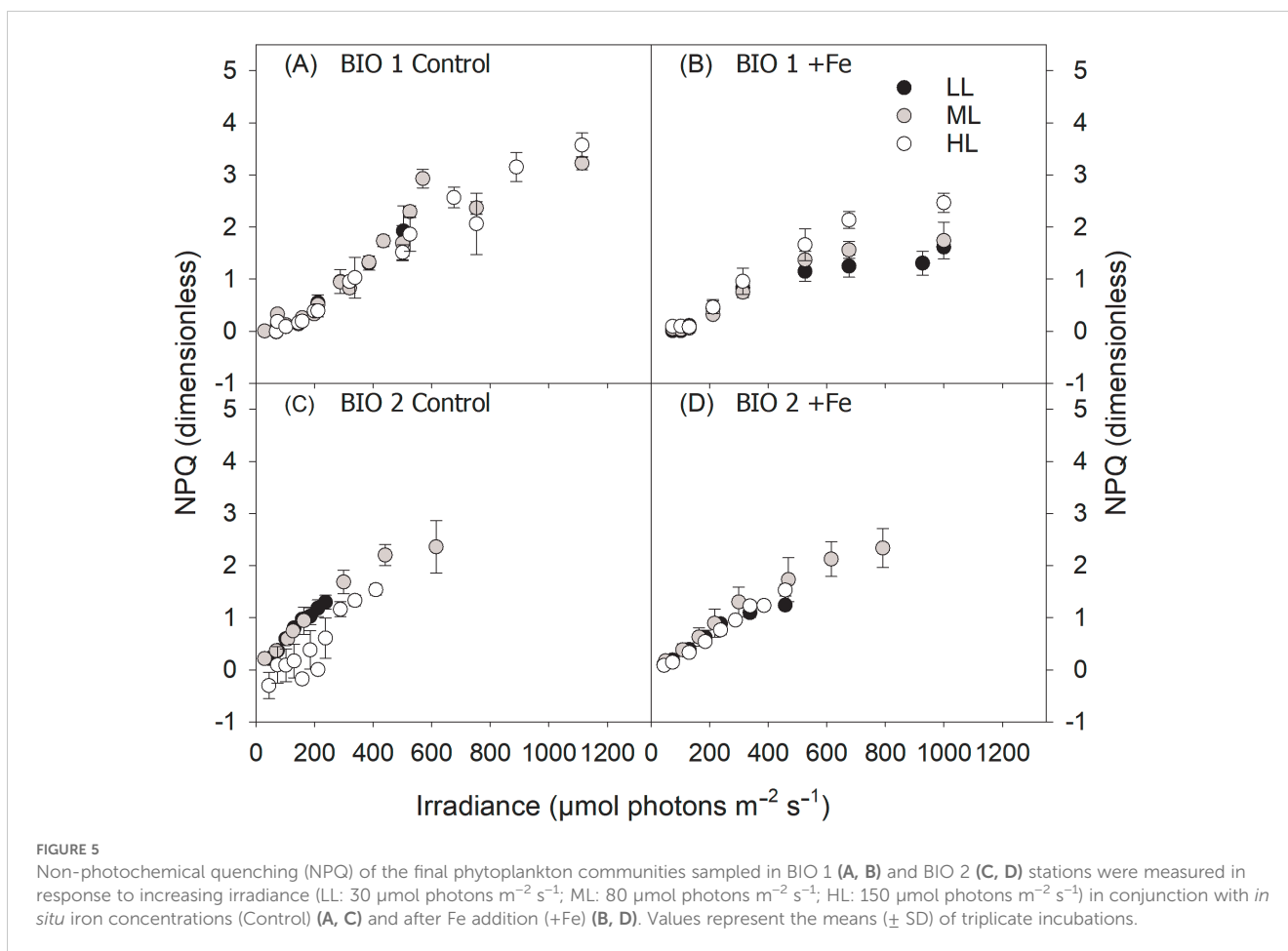


FIGURE 4

Absolute electron transport rates (ETRs) of the final phytoplankton communities sampled in BIO 1 (A, B) and BIO 2 (C, D) stations were measured in response to increasing irradiance (LL: 30 $\mu\text{mol photons m}^{-2} \text{s}^{-1}$; ML: 80 $\mu\text{mol photons m}^{-2} \text{s}^{-1}$; HL: 150 $\mu\text{mol photons m}^{-2} \text{s}^{-1}$) in conjunction with *in situ* iron concentrations (Control) (A, C) and after Fe addition (+Fe) (B, D). Values represent the means (\pm SD) of triplicate incubations.



Only when exposed to HL were ETR_{max} and POC production in the Control treatment of the BIO 1 community significantly increased (Table 2; Figure 1). In fact, POC production yielded maximum rates of $3.64 \mu\text{mol L}^{-1} \text{d}^{-1}$ under Control HL conditions, being 74% higher than the rate of the +Fe LL treatment ($2.09 \mu\text{mol L}^{-1} \text{d}^{-1}$; Figure 1A). Even without the addition of Fe, the combination of the Control treatment of the BIO 1 community with HL resulted in 5.6 times higher POC production rates than the Control LL treatment ($0.55 \mu\text{mol L}^{-1} \text{d}^{-1}$; Figure 1A). This clearly shows that HL neither led to light stress nor had a negative impact on the photosynthetic performance of the BIO 1 community. This is similar to the response of other natural phytoplankton communities (Joy-Warren et al., 2022; Vives et al., 2022; Latour et al., 2023) showing stimulation of POC rates with increasing light intensity even under low Fe availability. Hence, compared to the Fe-enriched community that yielded maximum POC production rates at ML, the Fe-limited BIO 1 phytoplankton community achieved maximum POC fixation rates only at HL (Figure 1A). Thus, only the supply of HL was able to alleviate the negative impact of Fe limitation on the BIO 1 community, demonstrating clearly that the BIO 1 community was limited by both Fe and light.

We also tested whether there was an increase in Fe demand at LL relative to the HL treatments, particularly under low Fe availability (Fe–light antagonism) as suggested by Sunda and Huntsman (1997). The observed lower $\mu\text{POC}_{\text{Con}}/\mu\text{POC}_{+\text{Fe}}$ ratios

at LL suggest a higher Fe requirement of the BIO 1 community (Table 4), which is consistent with the observations of previous studies (Viljoen et al., 2018; Joy-Warren et al., 2022), but in contrast to other Fe–light studies with Antarctic phytoplankton assemblages (Alderkamp et al., 2019; Vives et al., 2022; Latour et al., 2023). The reason for this discrepancy among studies could be the chosen light treatments since LL conditions were comparably high in our study ($30 \mu\text{mol photons m}^{-2} \text{s}^{-1}$), while our ML and HL treatments represented rather moderate light conditions (80 and $150 \mu\text{mol photons m}^{-2} \text{s}^{-1}$, respectively). In comparison, the studies that did not find this antagonistic relationship applied either very low light intensities ($2\text{--}6 \mu\text{mol photons m}^{-2} \text{s}^{-1}$; Latour et al., 2023) or very high irradiances ($331\text{--}512 \mu\text{mol photons m}^{-2} \text{s}^{-1}$; Alderkamp et al., 2019; $370\text{--}926 \mu\text{mol photons m}^{-2} \text{s}^{-1}$; Vives et al., 2022). Perhaps the larger light range that the phytoplankton was exposed to in the latter studies required potentially even stronger photoacclimation strategies, which, in contrast, lowered their Fe demand.

In our study, except for *Fragilariopsis*, which exhibited a light-dependent growth stimulation at each light level, growth of all other phytoplankton groups was enhanced only at HL ($150 \mu\text{mol photons m}^{-2} \text{s}^{-1}$) in the Control treatment of the BIO 1 community (Figure 2). Hoffmann et al. (2008) reported a negative impact on the growth of the SO diatoms *Chaetoceros dichchaeta* and *Actinocyclus* sp. in response to increasing light up to a moderate light level of $90 \mu\text{mol photons m}^{-2} \text{s}^{-1}$, while the growth of *C. debilis*

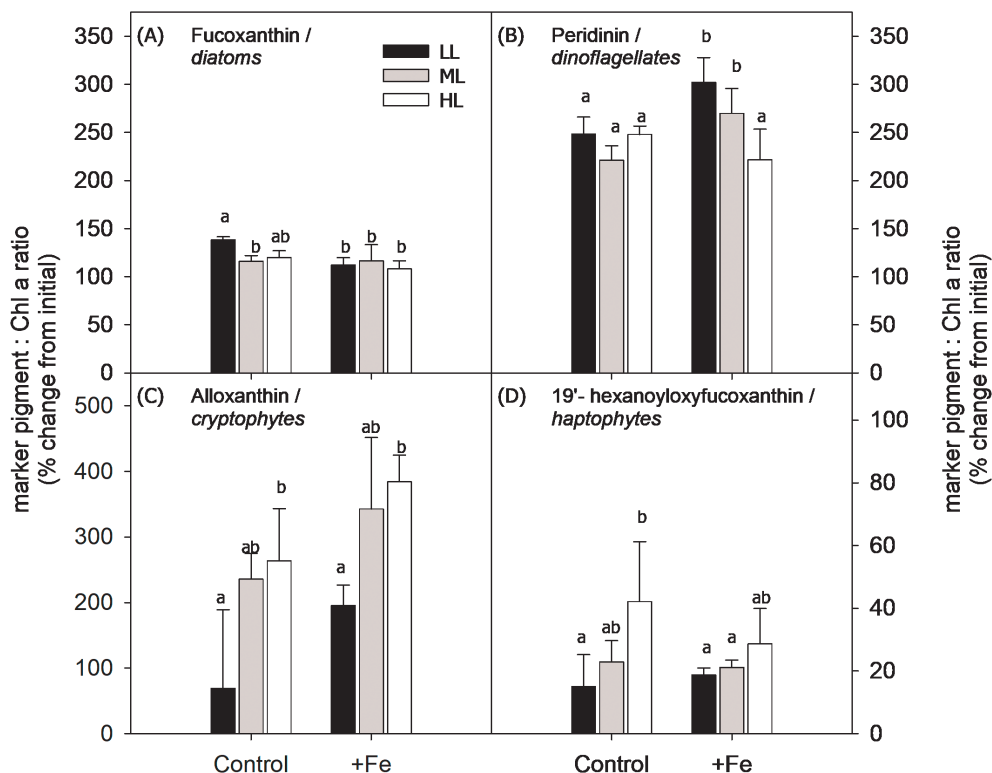


FIGURE 6

Ratio of marker pigment [fucoxanthin: diatoms (A); peridinin: dinoflagellates (B); alloxanthin: cryptophytes (C); 19'-hexanoxyfucoxanthin: haptophytes (D)] relative to Chl a was used as proxy to assess relative changes in the abundance of the major phytoplankton taxa in BIO 2 at the end of the incubation experiment. Using the calculated marker pigment to Chl a ratio at the initial community and at the end of the incubation, changes in the relative abundance of the target phytoplankton groups were calculated and given as % change from the marker pigment to Chl a ratio at the start of the experiment (>100% indicates positive growth). The phytoplankton community was grown at low light (LL; 30 $\mu\text{mol photons m}^{-2} \text{s}^{-1}$), middle light (ML; 80 $\mu\text{mol photons m}^{-2} \text{s}^{-1}$), and high light (HL; 150 $\mu\text{mol photons m}^{-2} \text{s}^{-1}$) in conjunction with *in situ* iron concentrations (Control) and after iron addition (+Fe). Values represent the means (\pm SD) of triplicate incubations. Significant differences between treatments are indicated by varying lowercase letters (*post-hoc* tests, $p < 0.05$).

remained unaffected. Moreover, Strzepek et al. (2012) showed either no or positive high light effects (ranging from 100 up to 280 $\mu\text{mol photons m}^{-2} \text{s}^{-1}$) on the growth of two Fe-limited Antarctic diatoms (*Proboscia inermis* and *Eucampia antarctica*, respectively). In contrast to ML, our study showed that the growth of all phytoplankton groups strongly benefitted from the HL supply, indicating that light limitation could be relieved under low Fe supply, as previously observed for Antarctic phytoplankton assemblages (Viljoen et al., 2018; Joy-Warren et al., 2022; Vives et al., 2022; Latour et al., 2023). It appears that the HL treatment of 150 $\mu\text{mol photons m}^{-2} \text{s}^{-1}$ provided optimal growth conditions for all community members. Based on our results, the growth of most members of the BIO 1 community was clearly Fe-light co-limited.

BIO 2: ML successfully relieved light limitation of the Fe-enriched BIO 2 community and promoted the highest POC production

Similar to the BIO 1 phytoplankton assemblage, positive light effects between LL and ML on POC production were found in the

+Fe treatments of the BIO 2 community (Figure 1B). Between LL and ML, the ratio of LH: LP declined, shifting the pigment ratio from a light absorption toward a more light-protective state (Figure 3B). Furthermore, σ_{PSII} and I_k increased between LL and ML (Table 2), indicating that more light was required for photosynthesis to become saturated. This photophysiological adjustment, however, allowed the cells to achieve higher ETR_{max} (Table 2) and POC production rates (Figure 1B) between LL and ML, indicating efficient linear electron cycling. Overall, this study shows that, as for the BIO 1 community, ML successfully relieved the light limitation of the BIO 2 community. With Fe enrichment, ML promoted the highest growth and POC fixation rates. In contrast to the diatom-dominated BIO 1 assemblage, the flagellate-dominated BIO 2 community underwent various photophysiological adjustments even after Fe addition under ML, corresponding to Fe-limiting conditions such as the increase in σ_{PSII} and more photoprotective pigments (Petrou et al., 2014; Vives et al., 2022; Alderkamp et al., 2019). This points toward the higher Fe requirement of SO flagellates than diatoms (Twining et al., 2004), as previously shown for the Antarctic cryptophyte *G. cryophila* relative to the diatom *Pseudo-nitzschia subcurvata* (Camoying et al., 2022).

When exposed to even higher irradiance (HL), POC production remained constant in the Fe-enriched BIO 2 community, with σ_{PSII} , I_k , and ETR_{max} being lowered between ML and HL (Table 2; Figure 4). The relative abundance of cryptophytes, however, was enhanced between LL and HL, suggesting that the higher light supply was beneficial for this group. Such positive light effects, especially of moderate light intensities under Fe-replete conditions on cryptophytes, have been observed before, both in laboratory studies with the cryptophyte *G. cryophila* (Trimborn et al., 2019; Camoying and Trimborn, 2023) and in field studies showing that cryptophytes are often associated with illuminated and stratified waters (Mendes et al., 2018; 2023). In contrast to the beneficial HL effects on cryptophytes, relative abundances of the dinoflagellates of the BIO 2 community declined from ML to HL under +Fe conditions, as indicated by the lowered peridinin:Chl *a* ratio (Figure 6B). This suggests that dinoflagellates benefit more from low and medium irradiances than from HL after Fe addition. Even though species composition was altered in response to the HL supply, this, however, did not change the overall productivity of the BIO 2 community. Hence, the BIO 2 community was most productive when grown in Fe-enriched and medium irradiances, indicating a successful relief of their Fe and light limitation. Similar to the BIO 1 community, the exposure of even higher irradiances did not lead to any further additional positive effects, suggesting light saturation and probably also a higher Fe demand, which potentially needed to be fulfilled in order to achieve even higher POC production by the flagellate-dominated BIO 2 community.

BIO 2: The Control treatment of the BIO 2 community responded to increasing light in the same manner as the Fe-enriched treatment

In contrast to BIO 1, in both the Control and +Fe treatments of the BIO 2 community, the LH:LP ratios decreased, while I_k and ETR_{max} were enhanced from LL to ML (Table 2), which in turn resulted in significantly higher POC production rate at ML (Figure 1B). Moreover, it needs to be noted that the supply of ML alone (without any Fe added) increased the POC production of the Control similarly high as that of the +Fe treatment under LL (Figure 1B). This indicates that the community was not only Fe-limited but light-limited as well and that the higher light availability alleviated the negative effects of Fe limitation in the Control. For BIO 2, σ_{PSII} and ETR_{max} decreased in the Control from ML to HL, but this did not result in reduced POC production, as rates remained the same between ML and HL, similar to the +Fe treatment. Since maximum POC production was achieved at ML after Fe addition, the BIO 2 phytoplankton community was clearly Fe–light co-limited.

As was observed for BIO 1, the BIO 2 assemblage also exhibited an increased demand for Fe at LL as shown by the lower $\mu POC_{Con}/\mu POC_{+Fe}$ ratio of the LL treatment compared to both ML and HL treatments (LL: 0.35 ± 0.09 vs. ML: 0.57 ± 0.06 and HL: 0.67 ± 0.05 ; Table 4). The $\mu POC_{Con}/\mu POC_{+Fe}$ ratios of the LL treatment of the

BIO 2 assemblage were also lower than those of the LL treatment of the BIO 1 community (Table 4), potentially indicating higher Fe requirement of the flagellate-dominated station. While SO phytoplankton are commonly known to increase their σ_{PSII} in response to Fe limitation (Strzepek et al., 2019), both communities in our study did not exhibit a strong Fe-dependent decrease in σ_{PSII} with Fe addition, and values at the end of the incubations were fairly similar between the two stations despite being composed of different phytoplankton assemblages (Table 2). The absence of this photophysiological adjustment may explain the increase in Fe demand of both communities under LL.

With respect to the community composition, aside from the strongly lowered relative abundance of haptophytes at the end of the incubation, the diatoms, cryptophytes, and dinoflagellates maintained positive growth throughout the course of the experiment (% change of pigment marker to Chl *a* ratio from the initial: >100% indicates positive growth; Figure 6). At the end of the incubation, the mixotrophic cryptophytes and dinoflagellates were most abundant, showing up to 300% and 250% increase, respectively. Since in the Control both the cryptophytes and haptophytes exhibited a similar increase in their relative abundance between LL and HL, this suggests that the dinoflagellates most likely were the ones to prey on haptophytes, causing their overall decline at the end of the incubation. In line with this, culture experiments with a novel dinoflagellate isolated from the Ross Sea (Gast et al., 2007) have shown the selective predation of the dinoflagellate on the Antarctic haptophyte *P. antarctica* (Sellers et al., 2014). In addition to potential predation effects, some HL effects were also observed. For instance, the relative abundance of diatoms significantly declined between LL and ML in the Control, indicating a susceptibility of diatoms to higher irradiances under Fe limitation, while positive HL effects were observed for the cryptophytes and haptophytes. Considering that our Fe–light experiments were conducted during late summer, it could also be that grazing of large-sized diatoms occurred prior to sampling and that much of the dFe in BIO 2 was recycled Fe. In the absence of Fe addition, the small-sized diatoms were potentially outcompeted by the flagellates in the Control treatment since regenerated Fe is more easily accessible to the latter (Boyd et al., 2012), in addition to the finding that haptophytes and cryptophytes are well-adapted to high irradiances (Trimborn et al., 2019; Camoying and Trimborn, 2023; Mendes et al., 2023).

Ecological implications

With the ongoing ocean acidification and global warming events, two scenarios are projected for the open ocean regions of the SO. The first scenario predicts the shallowing of the mixed layer depth (MLD) due to sea surface temperature warming and the subsequent melting of sea ice (Meijers, 2014). This would result in increased light availability to phytoplankton (Bopp et al., 2013) but would reduce the input of trace metals from deeper water layers (Bopp et al., 2001). The second scenario, in contrast, projects a poleward shift and strengthening of westerly winds (Meijers, 2014), and this is expected

to result in reduced light availability due to the deepening of the MLD and an increase in Fe input from deeper layers due to stronger water column mixing (Hauck et al., 2015). Based on the response of the diatom-dominated community in the open waters of the Drake Passage (BIO 1), under the first scenario with less Fe, but more light, POC production would only be enhanced when exposed to high light ($150 \mu\text{mol photons m}^{-2} \text{s}^{-1}$), but not at low and medium light (30 and $80 \mu\text{mol photons m}^{-2} \text{s}^{-1}$, respectively). With the second scenario of high Fe supply, but low light availability, POC production would also be enhanced. Hence, both scenarios would lead to increased growth and carbon production of the open ocean diatom-dominated community.

With regard to the coastal Antarctic region, climate change models project increased stratification due to melting ice and surface water freshening, thereby increasing the light available to phytoplankton together with higher nutrient inputs from the melting glaciers and sea ice (Deppeler and Davidson, 2017). Such a scenario of high light and high Fe availability would also lead to enhanced growth and carbon production of the flagellate-dominated coastal WAP community (BIO 2).

Climate change models predict an enhanced Fe input and light availability in the future SO, which would in turn result in an overall increase in net primary production and growth of SO phytoplankton (Henley et al., 2020). The results of our two field experiments corroborate the simulation outcomes of the SO models since we observed a significant enhancement in the POC production of the two distinct SO phytoplankton assemblages in response to medium irradiance ($80 \mu\text{mol photons m}^{-2} \text{s}^{-1}$) and high Fe supply. However, the degree of POC production increase would be higher in the diatom-dominated than flagellate-dominated community, which could be attributed to the lower Fe requirement of diatoms relative to flagellates. Exposure of SO phytoplankton communities to even higher light ($150 \mu\text{mol photons m}^{-2} \text{s}^{-1}$), however, would not lead to a further increase in POC production. Given the projected dominance of diatoms, carbon export of the open ocean regions of the SO would be enhanced, while that of coastal WAP waters would be reduced since small flagellates are said to be less efficient vectors for carbon export compared to the large, silica-containing diatoms (Armstrong et al., 2009; Ducklow et al., 2001). Moreover, the increase in the abundance of small flagellates could also have an impact on the distribution patterns of key SO grazers (krill and salps). For instance, krill are reported to prefer feeding on large-sized diatoms (Meyer and El-Sayed, 1983; Haberman et al., 2003), while salps, being non-selective feeders, are able to efficiently feed on small flagellates (Pakhomov et al., 2002). The potential shift in the dominance from krill to salps could result in a decreased availability of food to higher trophic organisms (i.e., seals, penguins, and whales; Henley et al., 2020), thus affecting the food web dynamics in the SO. Moreover, while flagellates may not be the preferred food of krill, they may serve as a rich source of recycled Fe due to their high cellular Fe content.

Data availability statement

The raw data supporting the conclusions of this article will be made available by the authors, without undue reservation.

Author contributions

MC: Formal analysis, Visualization, Writing – original draft, Writing – review & editing. FK: Investigation, Writing – review & editing. JS: Methodology, Writing – review & editing. FP: Methodology, Writing – review & editing. CH: Writing – review & editing. ST: Conceptualization, Funding acquisition, Investigation, Supervision, Writing – review & editing.

Funding

The author(s) declare financial support was received for the research, authorship, and/or publication of this article. FK, FP, and ST were funded by the Helmholtz Impulse Fond (HGF Young Investigators Group EcoTrace, VH-NG-901). MC was funded by the Katholischer Akademischer Ausländer-Dienst (KAAD) through a PhD scholarship.

Acknowledgments

We thank T. Brenneis for analyzing the POC samples and C. Völkner and D. Wilhelms-Dick for the ICP-MS measurements. We are grateful to M. Van Leeuwe for the insightful discussions on the interpretation of our HPLC marker pigment data. We acknowledge the support from the Open Access Publication Fund of the Alfred Wegener Institute, Helmholtz Centre for Polar and Marine Research. We also thank J. Heiden, R. Zimmerman, and P. Karitter for their assistance during field sampling. Lastly, we thank the cruise leader, captain, and crew of *RV Polarstern* during the PS97 expedition.

Conflict of interest

The authors declare that the research was conducted in the absence of any commercial or financial relationships that could be construed as a potential conflict of interest.

Publisher's note

All claims expressed in this article are solely those of the authors and do not necessarily represent those of their affiliated organizations, or those of the publisher, the editors and the reviewers. Any product that may be evaluated in this article, or claim that may be made by its manufacturer, is not guaranteed or endorsed by the publisher.

Supplementary material

The Supplementary Material for this article can be found online at: <https://www.frontiersin.org/articles/10.3389/fmars.2024.1441087/full#supplementary-material>

References

- Alderkamp, A. C., De Baar, H. J. W., Visser, R. J. W., and Arrigo, K. R. (2010). Can photoinhibition control phytoplankton abundance in deeply mixed water columns of the Southern Ocean? *Limnol. Oceanogr.* 55, 1248–1264. doi: 10.4319/lo.2010.55.3.1248
- Alderkamp, A. C., Kulk, G., Buma, A. G. J., Visser, R. J. W., Van Dijken, G. L., Mills, M. M., et al. (2012). The effect of iron limitation on the photophysiology of *Phaeocystis Antarctica* (Prymnesiophyceae) and *Fragilariopsis cylindrus* (Bacillariophyceae) under dynamic irradiance. *J. Phycol.* 48, 45–59. doi: 10.1111/j.1529-8817.2011.01098.x
- Alderkamp, A. C., Van Dijken, G. L., and Lowry, K. E. (2015). Fe availability drives phytoplankton photosynthesis rates during spring bloom in the Amundsen Sea Polynya, Antarctica. *Elementa* 3, 1–26. doi: 10.12952/journal.elementa.000043
- Alderkamp, A. C., Van Dijken, G. L., and Lowry, K. E. (2019). Effects of iron and light availability on phytoplankton photosynthetic properties in the Ross Sea. *Mar. Ecol. Prog. Ser.* 621, 33–50. doi: 10.3354/meps13000
- Andrew, S. M., Morell, H. T., Strzepek, R. F., Boyd, P. W., and Ellwood, M. J. (2019). Iron availability influences the tolerance of Southern Ocean phytoplankton to warming and elevated irradiance. *Front. Mar. Sci.* 6. doi: 10.3389/fmars.2019.00681
- Armstrong, R. A., Peterson, M. L., Lee, C., and Wakeham, S. G. (2009). Settling velocity spectra and the ballast ratio hypothesis. *Deep Sea Res. Part II Top. Stud. Oceanogr.* 56, 1470–1478. doi: 10.1016/j.dsr2.2008.11.032
- Arrigo, K. R. (2005). Marine microorganisms and global nutrient cycles. *Nature* 437, 349–355.
- Balaguer, J., Koch, F., Hassler, C., and Trimborn, S. (2022). Iron and manganese co-limit the growth of two phytoplankton groups dominant at two locations of the Drake Passage. *Commun. Biol.* 5, 1–12. doi: 10.1038/s42003-022-03148-8
- Behrenfeld, M. J., and Milligan, A. J. (2013). Photophysiological expressions of iron stress in phytoplankton. *Ann. Rev. Mar. Sci.* 5, 217–246. doi: 10.1146/annurev-marine-121211-172356
- Blain, S., Quéguiner, B., Armand, L., Belviso, S., Bombled, B., Bopp, L., et al. (2007). Effect of natural iron fertilization on carbon sequestration in the Southern Ocean. *Nature* 446, 1070–1074. doi: 10.1038/nature05700
- Blanco-Ameijeiras, S., Cabanes, D. J. E., Cable, R. N., Trimborn, S., Jacquet, S., Wiegmann, S., et al. (2020). Exopolymeric substances control microbial community structure and function by contributing to both C and Fe nutrition in Fe-limited Southern Ocean provinces. *Microorganisms* 8, 1–21. doi: 10.3390/microorganisms8121980
- Bopp, L., Monfray, P., Aumont, O., Dufresne, J.-L., LeTreut, H., Madec, G., et al. (2001). Potential impact of climate change on marine export production. *Glob. Biogeochem. Cyc.* 15, 81–99. doi: 10.1029/1999GB001256
- Bopp, L., Resplandy, L., Orr, J. C., Doney, S. C., Dunne, J. P., Gehlen, M., et al. (2013). Multiple stressors of ocean ecosystems in the 21st century: projections with CMIP5 models. *Biogeosciences* 10, 6225–6245. doi: 10.5194/bg-10-6225-2013
- Boyd, P. W., Strzepek, R., Chiswell, S., Chang, H., DeBruyn, J. M., Ellwood, M., et al. (2012). Microbial control of diatom bloom dynamics in the open ocean. *Geophys. Res. Lett.* 39, L18601. doi: 10.1029/2012GL053448
- Boyd, P. W., Watson, A. J., and Law, C. S. (2000). A mesoscale phytoplankton bloom in the polar Southern Ocean stimulated by iron fertilization. *Nature* 407, 695–702. doi: 10.1038/35037500
- Camoying, M. G., Bischof, K., Geuer, J. K., Koch, B. P., and Trimborn, S. (2022). In contrast to diatoms, cryptophytes are susceptible to iron limitation, but not to ocean acidification 174, 1–16. doi: 10.1111/ppl.13614
- Camoying, M. G., and Trimborn, S. (2023). Physiological response of an Antarctic cryptophyte to increasing temperature, CO₂, and irradiance. *Limnol. Oceanogr.* 2100, 1–15. doi: 10.1002/lno.12392
- Cutter, G., Casciotti, K., Croot, P., Geibert, W., Heimbürger, L.-E., Lohan, M., et al. (2017). *Sampling and Sample-handling Protocols for GEOTRACES Cruises* (Toulouse, France: GEOTRACES International Project Office). Available at: <http://www.geotraces.org/images/stories/documents/intercalibration/Cookbook.pdf>.
- Deppeler, S. L., and Davidson, A. T. (2017). Southern ocean phytoplankton in a changing climate. *Front. Mar. Sci.* 4. doi: 10.3389/fmars.2017.00040
- Ducklow, H. W., Steinberg, D. K., and Buesseler, K. O. (2001). Upper ocean carbon export and the biological pump. *Oceanography* 14, 50–58. doi: 10.5670/oceanog.2001.06
- Falkowski, P. G., and Raven, J. A. (2007). *Aquatic photosynthesis: (Second edition) (STU-student edition)* (Princeton University Press). Available at: <http://www.jstor.org/stable/j.ctt4cgbxs>.
- Feng, Y., Hare, C. E., Rose, J. M., et al. (2010). Interactive effects of iron, irradiance and CO₂ on ross sea phytoplankton. *Deep. Res. Part I Oceanogr. Res. Pap.* 57, 368–383. doi: 10.1016/j.dsr.2009.10.013
- Gast, R. J., Moran, D. M., Dennett, M. R., and Caron, D. A. (2007). Kleptoplasty in an Antarctic dinoflagellate: caught in evolutionary transition? *Environ. Microbiol.* 9, 39–45. doi: 10.1111/j.1462-2920.2006.01109.x
- Haberman, K. L., Ross, R. M., and Quetin, L. B. (2003). Diet of the Antarctic krill (*Euphausia superba* Dana): II. Selective grazing in mixed phytoplankton assemblages. *J. Exp. Mar. Biol. Ecol.* 283, 97–113. doi: 10.1016/S0022-0981(02)00467-7
- Hathorne, E. C., Haley, B., Stichel, T., Grasse, P., Zieringer, M., and Frank, M. (2012). Online preconcentration ICP-MS analysis of rare earth elements in seawater. *Geochemistry Geophysics Geosystems* 13. doi: 10.1029/2011GC003907
- Hauck, J., Völker, C., Wolf-Gladrow, D. A., Laufkötter, C., Vogt, M., Aumont, O., et al. (2015). On the Southern Ocean CO₂ uptake and the role of the biological carbon pump in the 21st century. *Glob. Biogeochem. Cycles* 29, 1451–1470. doi: 10.1002/2015GB005140
- Heiden, J. P., Bischof, K., and Trimborn, S. (2016). Light intensity modulates the response of two Antarctic diatom species to ocean acidification. *Front. Mar. Sci.* 3. doi: 10.3389/fmars.2016.00260
- Heiden, J. P., Völkner, C., Jones, E. M., et al. (2019). Impact of ocean acidification and high solar radiation on productivity and species composition of a late summer phytoplankton community of the coastal western antarctic peninsula. *Limnol. Oceanogr.* 64, 1716–1736. doi: 10.1002/lno.11147
- Henley, S. F., Cavan, E. L., Fawcett, S. E., Kerr, R., Monteiro, T., Sherrell, R. M., et al. (2020). Changing biogeochemistry of the southern ocean and its ecosystem implications. *Front. Mar. Sci.* 7. doi: 10.3389/fmars.2020.00581
- Hoffmann, L. J., Peeken, I., and Lochte, K. (2008). Iron, silicate, and light co-limitation of three Southern Ocean diatom species. *Polar Biol.* 31, 1067–1080. doi: 10.1007/s00300-008-0448-6
- Huot, Y., and Babin, M. (2010). “Overview of fluorescence protocols: theory, basic concepts, and practice,” in *Chlorophyll a fluorescence in aquatic sciences: Methods and applications*. Eds. D. J. Suggett, M. A. Borowitzka and O. Prášil (Berlin: Springer). doi: 10.1007/978-90-481-9268-7
- Joy-Warren, H. L., Alderkamp, A. C., and van Dijken, G. L. (2022). Springtime phytoplankton responses to light and iron availability along the western Antarctic Peninsula. *Limnol. Oceanogr.* 67, 1–16. doi: 10.1002/lno.12035
- Koch, F., Beszteri, S., Harms, L., and Trimborn, S. (2019). The impacts of iron limitation and ocean acidification on the cellular stoichiometry, photophysiology, and transcriptome of *Phaeocystis Antarctica*. *Limnol. Oceanogr.* 64, 357–375. doi: 10.1002/lno.11045
- Koch, F., and Trimborn, S. (2019). Limitation by Fe, Zn, Co, and B₁₂ results in similar physiological responses in two Antarctic phytoplankton species. *Front. Mar. Sci.* 6. doi: 10.3389/fmars.2019.00514
- Latour, P., Eggins, S., and van der Merwe, P. (2023). Characterization of a Southern Ocean deep chlorophyll maximum: Response of phytoplankton to light, iron, and manganese enrichment. *Limnol. Oceanogr. Lett.* 9, 145–154. doi: 10.1002/lo.210366
- Lee, Y., Jung, T. W., Kim, E. J., and Park, J. (2022). Phytoplankton growth rates in the Amundsen Sea (Antarctica) during summer: The role of light. *Environ. Res.* 207. doi: 10.1016/j.envres.2021.112165
- Luxem, K. E., Ellwood, M. J., and Strzepek, R. F. (2017). Intraspecific variability in *Phaeocystis Antarctica*'s response to iron and light stress. *PLoS One* 12 (7), e0179751. doi: 10.1371/journal.pone.0179751
- Mackey, M. D., Mackey, D. J., Higgins, H. W., and Wright, S. W. (1996). CHEMTAX - A program for estimating class abundances from chemical markers: Application to HPLC measurements of phytoplankton. *Mar. Ecol. Prog. Ser.* 144, 265–283. doi: 10.3354/meps144265
- Maldonado, M. T., Boyd, P. W., Harrison, P. J., and Price, N. M. (1999). Co-limitation of phytoplankton growth by light and Fe during winter in the NE subarctic Pacific ocean. *Deep. Res. Part II Top. Stud. Oceanogr.* 46, 2475–2485. doi: 10.1016/S0967-0645(99)00072-7
- Marchetti, A., Maldonado, M. T., Lane, E. S., and Harrison, P. J. (2006). Iron requirements of the pennate diatom *Pseudo-nitzschia* Comparison of oceanic (high-nitrate, low-chlorophyll waters) and coastal species. *Limnology Oceanography* 51, 2092–2101. doi: 10.4319/lo.2006.51.5.2092
- Martin, J. H., Fitzwater, S. E., and Gordon, R. M. (1990). Iron deficiency limits phytoplankton growth in antarctic waters. *Global Biogeochem. Cycles* 4, 5–12. doi: 10.1029/GB004i001p00005
- Meijers, A. J. S. (2014). The Southern Ocean in the coupled model intercomparison project phase 5. *Phil. Trans. R. Soc A* 372, 20130296. doi: 10.1098/rsta.2013.0296
- Mendes, C. R. B., Costa, R. R., Ferreira, A., Jesus, B., Tavano, V. M., Dotto, T. S., et al. (2023). Cryptophytes: An emerging algal group in the rapidly changing antarctic peninsula marine environments. *Glob. Change Biol.* 29, 1791–1808. doi: 10.1111/gcb.16602
- Mendes, C. R. B., Tavano, V. M., Dotto, T. S., Kerr, R., de Souza, M. S., Garcia, C. A. E., et al. (2018). New insights on the dominance of cryptophytes in antarctic coastal waters: A case study in Gerlache Strait. *Deep. Res. Part II Top. Stud. Oceanogr.* 149, 161–170. doi: 10.1016/j.dsr2.2017.02.010
- Meyer, M. A., and El-Sayed, S. Z. (1983). Grazing of *Euphausia superba* Dana on natural phytoplankton populations. *Polar Biol.* 1, 193–197. doi: 10.1007/BF00443187
- Mitchell, B. G., Brody, E. A., Holm-Hansen, O., McClain, C., and Bishop, J. (1991). Light limitation of phytoplankton biomass and macro-nutrient utilization in the southern ocean. *Limnology Oceanography* 36 (8), 1662–1677.
- Moore, C. M., Seeyave, S., Hickman, A. E., Allen, J. T., Lucas, M. I., Planquette, H., et al. (2007). Iron-light interactions during the CROZET natural iron bloom and EXPORT experiment (CROZEX) I: phytoplankton growth and photophysiology. *Deep-Sea Res. II Top. Stud. Oceanogr.* 54, 2045–2065. doi: 10.1016/j.dsr2.2007.06.011

- Oxborough, K., Moore, C. M., Suggett, D. J., Lawson, T., Chan, H. G., and Geider, R. J. (2012). Direct estimation of functional PSII reaction center concentration and PSII electron flux on a volume basis: A new approach to the analysis of fast repetition rate fluorometry (FRRF) data. *Limnol. Oceanogr. Methods* 10, 142–154. doi: 10.4319/lom.2012.10.142
- Pakhomov, E. A., Froneman, P. W., and Perissinotto, R. (2002). Salp/krill interactions in the Southern Ocean: Spatial segregation and implications for the carbon flux. *Deep Sea Res. II* 49, 1881–1907. doi: 10.1016/S0967-0645(02)00017-6
- Pausch, F., Koch, F., Hassler, C., Bracher, A., Bischof, K., and Trimbom, S. (2022). Responses of a natural phytoplankton community from the Drake Passage to two predicted climate change scenarios. *Front. Mar. Sci.* 9, 1–18. doi: 10.3389/fmars.2022.759501
- Peers, G., and Price, N. M. (2004). A role for manganese in superoxide dismutases and growth of iron-deficient diatoms. *Limnol. Oceanogr.* 49, 1774–1783. doi: 10.4319/lo.2004.49.5.1774
- Petrou, K., Hassler, C. S., Doblin, M. A., Shelly, K., Schoemann, V., van den Enden, R., et al. (2011). Iron-limitation and high light stress on phytoplankton populations from the Australian Sub-Antarctic Zone (SAZ). *Deep. Res. Part II Top. Stud. Oceanogr.* 58, 2200–2211. doi: 10.1016/j.dsr2.2011.05.020
- Petrou, K., Trimbom, S., Rost, B., Ralph, P. J., and Hassler, C. S. (2014). The impact of iron limitation on the physiology of the Antarctic diatom *Chaetoceros simplex*. *Mar. Biol.* 161, 925–937. doi: 10.1007/s00227-014-2392-z
- Ralph, P. J., and Gademann, R. (2005). Rapid light curves: a powerful tool to assess photosynthetic activity. *Aquat. Bot.* 82, 222–237. doi: 10.1016/j.aquabot.2005.02.006
- Rapp, I., Schlosser, C., Rusiecka, D., Gledhill, M., and Achterberg, E. P. (2017). Automated preconcentration of Fe, Zn, Cu, Ni, Cd, Pb, Co, and Mn in seawater with analysis using high-resolution sector field inductively-coupled plasma mass spectrometry. *Analytica Chim. Acta* 976, 1–13. doi: 10.1016/j.aca.2017.05.008
- Raven, J. A. (1990). Predictions of Mn and Fe use efficiencies of phototrophic growth as a function of light availability for growth and of C assimilation pathway. *New Phytol.* 116, 1–18. doi: 10.1111/j.1469-8137.1990.tb00505.x
- Ryan-Keogh, T. J., DeLizo, L. M., Smith, W. O., Sedwick, P. N., McGillicuddy, D. J., Moore, C. M., et al. (2017). Temporal progression of photosynthetic-strategy in phytoplankton in the Ross Sea, Antarctica. *J. Mar. Syst.* 166, 87–96. doi: 10.1016/j.jmarsys.2016.08.014
- Sellers, C. G., Gast, R. J., and Sanders, R. W. (2014). Selective feeding and foreign plastid retention in an Antarctic dinoflagellate. *J. Phycol.* 50, 1081–1088. doi: 10.1111/jpy.12240
- Strzepek, R. F., Boyd, P. W., and Sunda, W. G. (2019). Photosynthetic adaptation to low iron, light, and temperature in Southern Ocean phytoplankton. *Proc. Natl. Acad. Sci. U.S.A.* 116, 4388–4393. doi: 10.1073/pnas.1810886116
- Strzepek, R. F., Hunter, K. A., Frew, R. D., Harrison, P. J., and Boyd, P. W. (2012). Iron-light interactions differ in Southern Ocean phytoplankton. *Limnol. Oceanogr.* 57, 1182–1200. doi: 10.4319/lo.2012.57.4.1182
- Suggett, D. J., MacIntyre, H. L., and Geider, R. J. (2004). Evaluation of biophysical and optical determinations of light absorption by photosystem II in phytoplankton. *Limnol. Oceanogr. Methods* 2, 316–332. doi: 10.4319/lom.2004.2.316
- Sunda, W. G., and Huntsman, S. A. (1997). Interrelated influence of iron, light and cell size on marine phytoplankton growth. *Nature* 390, 389–392. doi: 10.1038/37093
- Sunda, W., Swift, D., and Huntsman, S. (1991). Low iron requirement for growth in oceanic phytoplankton. *Nature* 351, 55–57. doi: 10.1038/351055a0
- Trimbom, S., Thoms, S., Bischof, K., and Beszteri, S. (2019). Susceptibility of two Southern Ocean phytoplankton key species to iron limitation and high light. *Front. Mar. Sci.* 6. doi: 10.3389/fmars.2019.00167
- Twining, B. S., Baines, S. B., Fisher, N. S., and Landry, M. R. (2004). Cellular iron contents of plankton during the Southern Ocean Iron Experiment (SOFEX). *Deep. Res. Part I Oceanogr. Res. Pap.* 51, 1827–1850. doi: 10.1016/j.dsr.2004.08.007
- Van Leeuwe, M., and Stefels, J. (1998). Effects of iron and light stress on the biochemical composition of antarctic Phaeocystis sp. (Prymnesiophyceae). II. Pigment composition. *J. Phycol.* 503, 496–503. doi: 10.1046/j.1529-8817.1998.340486.x
- Viljoen, J. J., Philibert, R., Van Horsten, N., Mtshali, T., Roychoudhury, A. N., Thomalla, S., et al. (2018). Phytoplankton response in growth, photophysiology and community structure to iron and light in the Polar Frontal Zone and Antarctic waters. *Deep Sea Res. Part I Oceanogr. Res. Pap.* 141, 118–129. doi: 10.1016/j.dsr.2018.09.006
- Vives, C. R., Schallenberg, C., Stratton, P. G., and Westwood, K. J. (2022). Iron and light limitation of phytoplankton growth off East Antarctica. *J. Mar. Syst.* 234, 103774. doi: 10.1016/j.jmarsys.2022.103774
- Wright, S. W., and Van den Enden, R. L. (2000). Phytoplankton community structure and stocks in the East Antarctic marginal ice zone (BROKE survey, January–March 1996) determined by CHEMTAX analysis of HPLC pigment signatures. *Deep. Res. Part II Top. Stud. Oceanogr.* 47, 2363–2400. doi: 10.1016/S0967-0645(00)00029-1
- Ye, Y., Sunda, W. G., Hong, H., and Shi, D. (2023). Interrelated influence of iron, light, and CO₂ on carbon fixation in a Southern Ocean diatom. *Limnol. Oceanogr.* 68, 1504–1516. doi: 10.1002/lno.12360